A new calix[4]arene-bis(crown ether) derivative displaying an improved caesium over sodium selectivity: molecular dynamics and experimental investigation of alkali-metal ion complexation

Véronique Lamare,*[a] Jean-François Dozol,[a] Saowarux Fuangswasdi,[b] Françoise Arnaud-Neu,[b] Pierre Thuéry,[c] Martine Nierlich,[c] Zouhair Asfari[d] and Jacques Vicens[d]

[a] *CEA CADARACHE, DESD/SEP, F-13108 St-Paul Lez Durance, Cedex, France*
[b] *ECPM, Laboratoire de Chimie Physique, UMR 7512 du CNRS, 1 rue Blaise Pascal, F-67008 Strasbourg, France*
[c] *CEA SACLAY, DSM/SCM, F-91191 Gif-sur-Yvette, France*
[d] *ECPM, Laboratoire de Chimie Analytique et Minérale, UMR 7512 du CNRS, 1 rue Blaise Pascal, F-67008 Strasbourg, France*

Received (in Cambridge) 27th August 1998, Accepted 26th November 1998

In the light of computational studies suggesting enhanced cation-binding abilities for various benzo derivatives of calix[4]arene-bis-crown-6 macrocycles, the synthesis and properties of one of these ligands, **BC6B2**, have been investigated. In this compound, di(1,2-phenylene)-annelated glycolic chains link the 1,3- and 2,4-phenyl rings of the calixarene, thereby forcing it into the 1,3-alternate conformation. The detailed structures of **BC6B2**·CH_3NO_2 **1** and $Cs_2(NO_3)_2$**BC6B2**·$CHCl_3$·H_2O **2** have been established by X-ray crystallography. Studies of coordination and solvent extraction of the alkali-metal ions have been used to compare this ligand with a number of related systems known previously.

Introduction

As reflected in a burgeoning literature, studies of chemical separation techniques and the design and synthesis of new extraction reagents have gained worldwide impetus in recent years.[1–3] In part, this impetus results from greater concerns for the environment, energy savings and recycling at the industrial level. It is also a result of the rise of the field of "supramolecular chemistry", which has provided a variety of new reagents with the capacity to substantially improve the selectivity and efficiency of many separation techniques.[4] Solvent extraction is one of the more prominent of these techniques and in the field of nuclear waste treatment it is of special interest for the selective elimination of caesium (as the radionuclides ^{135}Cs and ^{137}Cs).[5] The element may be present as Cs^+ cation in trace amounts in different types of aqueous solutions: solutions generated from spent fuel reprocessing are acidic and contain either fission products or, as in the case of evaporator concentrates, high concentrations of sodium nitrate.[6] Other high-salinity liquid wastes are basic and may contain significant amounts of potassium nitrate along with the sodium salt, as in the case of solutions stored at the Hanford depository.[7] The achievement of a very high selectivity for caesium over the other alkali-metal cations, especially sodium but to some extent potassium, is a major goal of efforts to use extraction to diminish the volume of radioactive waste ultimately to be disposed of in geological repositories.[2]

The rich coordination chemistry of the calixarenes includes a strong affinity of particular derivatives for the alkali metal cations and a high lipophilicity for the complexes.[8–10] Our own earlier work, for example, has demonstrated in addition that materials given the trivial name "calixbiscrowns" can be remarkably selective in their binding and transport of the alkali metal cations.[11–14] This family of receptors, in which calix[4]arene is forced into the "1,3-alternate" conformation by glycolic chain links between the phenolic oxygen atoms of the 1,3 and 2,4 phenyl rings, have been found, in the cases where the newly formed crown ether loops contain six oxygen atoms, to be suitable ligands for the removal of caesium ions from both acidic and basic nuclear wastes highly concentrated in sodium ions.[7,15–17] These ligands, designated by the acronym **BC6** (for bis-crown-6; followed, as shown later, by other letters indicating the nature and number of any substituents within the crown ether loops), are a primary subject of our continuing studies of selective complexation of alkali-metal cations through solution equilibrium measurements[18,19] and single-crystal X-ray diffraction structure determinations.[20–24] Much work has also been done on dialkyloxycalix[4]arene mono-crown derivatives, involving synthesis, X-ray crystal structures, and study of the calixarene conformation or crown size on the complexation and extracting properties towards alkali cations.[25–28]

Earlier computational studies of both mono- and bis-crown derivatives of calix[4]arene, considered in the gas phase and solution or at immiscible solvent interfaces, were devoted to the truly glycolic systems with simple ethylene spacers between the ligating oxygen atoms. The conclusions drawn from these works were that for larger cations, size complementarity of the polyether loop and the cation was a dominant factor but that for smaller cations, such as sodium, solvation effects were more important, since there was not enough affinity with the ligand to overcome the high desolvation energy upon complexation.[29–34] A recent publication has also shown that the calculated Cs^+/Na^+ extraction selectivity in chloroform decreases as the water content in the organic phase increases.[35] The possible effects of modification of the spacer groups were not considered. This and in particular the introduction of aromatic spacers, has in fact been the focus of our computational work and we were encouraged by the fact that the very first experimental studies of a calix[4]bis-crown-6 bearing a single aromatic spacer substituent within each crown loop showed this ligand to extract caesium more efficiently than its unsubstituted analogue and to do so with a higher Cs^+/Na^+ selectivity.[16]

Our initial simulations involved the application of molecular

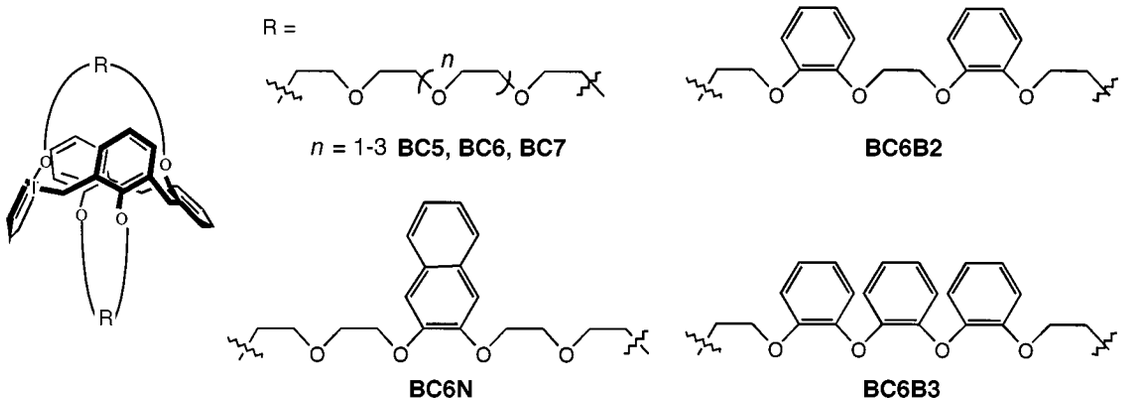

Fig. 1 1,3-Alt-calix[4]arene-bis-crowns modelled by MD and TI/MD simulations.

dynamics (MD) calculations in a vacuum and in water as well as free-energy-perturbation calculations (MD/FEP). They were applied to several **BC6** derivatives in which the central ethylene link of the crown loops was replaced by 1,2-, 1,3- or 1,4-phenylene units, and the qualitative criterion used to assess the ligands was the complementarity of the crown unit and the cation as indicated by the MD simulations in a vacuum (intrinsic complementarity) and in a water "box".[36,37] The possible enhancement of the desired properties, as revealed for the 1,2-phenylene species, encouraged us to perform further simulations for **BC6** derivatives with additional 1,2-phenylene units in the ring and the promising results obtained for the molecules bearing two or three aromatic spacers within the crown units (Fig. 1; **BC6B2** and **BC6B3**) led us to undertake their synthesis and practical evaluation.

Thus, we report herein the results of MD simulations, in a vacuum and in water, for calix[4]arene bis-crown derivatives used to calibrate the force field (validation of the charge set) and then the predicted properties for **BC6B2** and **BC6B3**. Additional calculations of free-energy derivatives with respect to the non-bonded parameters for the cations and of cation mutations within the calixarene–cation complex have been used to provide a qualitative insight into the origins of ligand selectivity. As an experimental evaluation of the validity of the predictions, we describe the synthesis of the calixcrown **BC6B2** which has been characterised through determination of crystal structure, and in quantitative equilibrium studies of alkali-metal ion extraction and complexation.

Results and discussion

Molecular modelling

Molecular dynamics simulations. MD simulations were performed on the alkali-metal ion complexes in a vacuum and in an explicit aqueous phase to evaluate the intrinsic stability of the complexes, the host–guest complementarity and the influence of a water-molecule environment upon these properties. These calculations are very sensitive to the non-bonded interaction parameters of the force-field equation, particularly the atomic charge sets on the calixarene and the van der Waals parameters of the cations. The van der Waals parameters of the alkali-metal cations have been calibrated by Aqvist to reproduce the free energies of hydration[38] and these constitute a widely-used set[29–37,39,40] but the choice of atomic charges is not straightforward for molecules as large as the calixarenes, for which it is conventional to break the molecule up into small components and calculate the charges either from *ab initio* electrostatic potentials or through cruder procedures. Of several charge sets used so far in calixcrown studies or in those of 1,2-phenylene-substituted crown ethers,[41] none could fully describe the series of calixarenes involved in the present work. Thus, a simple method was chosen involving MNDO scaled charges[42] which enabled the calculation of point charges without the necessity of dividing the calixarene into several parts. Validation of this charge set towards more polar MNDO/ESP charges has been recently performed on 1,3-alt-dioctyloxycalix[4]arene-C6B2, a monocrown analogue of **BC6B2**, for which X-ray crystal structures of CsPic and $KClO_4$–H_2O complexes were determined.[43] To finally evaluate the ligands, the well known concept of host–guest complementarity,[44] which involves assessment of the steric and electrostatic fit of host and guest, was used.

The intended use of the calixcrown ligands being studied was in liquid–liquid extraction experiments where the cation to be extracted is initially present in an aqueous phase and the ligand in an immiscible organic phase. A criterion of complementarity is thus the ability of the calixcrown to provide a coordination environment similar to that of the hydration shell of the cation. Part of this environment (number of donor atoms and their statistical distance to the cation) can be easily modelled by the summation of the radial distribution functions (rdfs) of the oxygen atom donor sites, $rdfO_C$, collected during MD simulations, and their comparison with the rdf of the water oxygen atoms, $rdfO_W$, around the "free" cation under similar simulation conditions.[39] Fig. 2 shows some examples of the rdf curves computed from MD simulations in vacuum. As an effective summary of the curves obtained for all the systems being studied, values of $\langle d(M^+–O_C)\rangle$, average of the 5 to 7 single $d(M^+–O_C)$ distances occurring during each MD run, are given in Table 1. This parameter provides a simple and useful interpretation of the rdf curves, although some information such as the fluctuations in single $d(M^+–O_C)$ distances is lost.

From simulations in a vacuum in the absence of a counter-anion, it seems that **BC6N** (where **N** denotes a 2,3-disubstituted naphthalene unit), **BC6B2** (Fig. 3) and **BC6B3** provide an excellent complementarity for Cs^+. **BC6** is slightly too large for a perfect fit and **BC5** is too small, though it does provide a good fit for Rb^+ and K^+. Calix[4]arene-crown-6 ligands bearing 1,2-phenylene groups show appropriate $rdfO_C$ curves for Rb^+ but the peak maximum is not quite ideal and $\langle d(Rb^+–O_C)\rangle$ is too large, with a significant dispersion of the single $d(M^+–O_C)$ values. These discrepancies are greater for K^+ and there is even poorer complementarity for Na^+, for which $rdfO_C$ curves show one peak with an integral ranging between 3 and 4 atoms, with the additional O_C atoms located in the second coordination shell.

In water, most of the complexes built without counter-ions are hydrated (Table 2), though adoption of a central position can render Na^+ inaccessible to solvent, as is also the case for K^+ in **BC6B3**. Coordination of a water molecule also improves the complementarity between Cs^+ and the substituted **BC6** ligands. The same is true for Rb^+ and K^+ with **BC5**.

Introduction of a counter anion (*e.g.*, NO_3^-) into the simulation system gives rise to a major electrostatic interaction

Table 1 Distances $\langle d(M^+–O_C)\rangle$ and $\langle d(C–O_C)\rangle$ (for empty crowns) during 500 ps of MD run in a vacuum or 100 ps in water (average of the single time averages)

	BC5	BC6B3	BC6B2	BC6N	BC6	$d(M^+–O_w)^a$	$d(M^+–O_w)_{exp}{}^b$
$\langle d(M^+–O_C)\rangle_{vac}{}^c$							
Cs^+	3.01(11)	**3.18(13)**	**3.15(9)**	**3.22(10)**	3.30(14)	**3.2**	3.13(7)
Rb^+	**2.95(14)**	3.12(21)	3.14(17)	3.16(14)	3.24(22)	**2.9**	2.88
K^+	2.93(17)	3.09(30)	3.04(9)	3.14(19)	3.32(34)	**2.8**	2.79(8)
Na^+	3.09(48)[d]	3.06(57)	3.11(73)	3.26(81)	3.45(81)[d]	**2.5**	3.35(6)
$CsNO_3$	3.05(5)	3.36(9)	3.33(4)	3.42(10)	3.47(13)		
$RbNO_3$	**2.98(5)**	3.32(19)	3.26(30)	3.38(20)	3.48(25)		
KNO_3	**2.94(5)**	3.27(19)	3.27(37)	3.38(61)	3.46(28)		
$NaNO_3$	2.83(14)	3.23(29)	3.14(78)	3.15(1.03)	3.47(35)		
$\langle d(M^+–O_C)\rangle_{wat}{}^e$							
Cs^+	3.00(4)	**3.22(9)**	**3.19(3)**	**3.21(3)**	3.29(10)		
Rb^+	**2.90(5)**	3.23(8)	3.28(23)	3.17(19)	3.40(23)		
K^+	**2.88(3)**	3.06(35)	3.13(14)	3.21(14)	3.66(81)		
Na^+	3.07(36)	3.02(62)	3.02(70)	3.64(70)[f]	3.21(91)		
$\langle d(C–O_C)\rangle_{vac}{}^g$							
Empty crown[h]	2.87(36)	3.04(35)	3.24(39)	3.25(41)	3.37(44)		
Free calixarene[i]	2.96(38)	3.16(47)	3.26(50)	3.36(40)	3.50(50)		

[a] $d(M^+–O_w)$, distance cation–O_{water} at the maximum of the first hydration peak of the rdf collected during 20 ps of MD run for the free cation in water. [b] Ref. 62. [c] $\langle d(M^+–O_C)\rangle$ (Å): average of the 5 to 6 individual $d(M^+–O)$ time averages during the MD sampling at 300 K. ( ) fluctuation. [d] Average calculated on 100 ps, on a longer sampling Na^+ oscillates between both crowns. [e] Averages calculated on stabilized structures if hydration occurs during the MD. [f] Average calculated over 80 ps, decomplexation occurs at 85 ps. [g] C: mass center of the oxygen atoms of the crown. $\langle d(C–O_C)\rangle$ (Å): average of the 5 to 6 $d(C–O)$ distances. [h] Average on the 8 simulations performed at 300 K on the mononuclear complex with and without counterion. An additional sampling for **BC6N** of 1 ns at 500 K gives $\langle d(C–O_C)\rangle = 3.22(37)$ for the empty crown. [i] Sampling time at 300 K: 500 ps for **BC5** and **BC6B3**, 1 ns for **BC6B2** and **BC6**. At 500 K: 1 ns for **BC6N**. In bold characters: closest values compared to $d(M^+–O_w)$.[a]

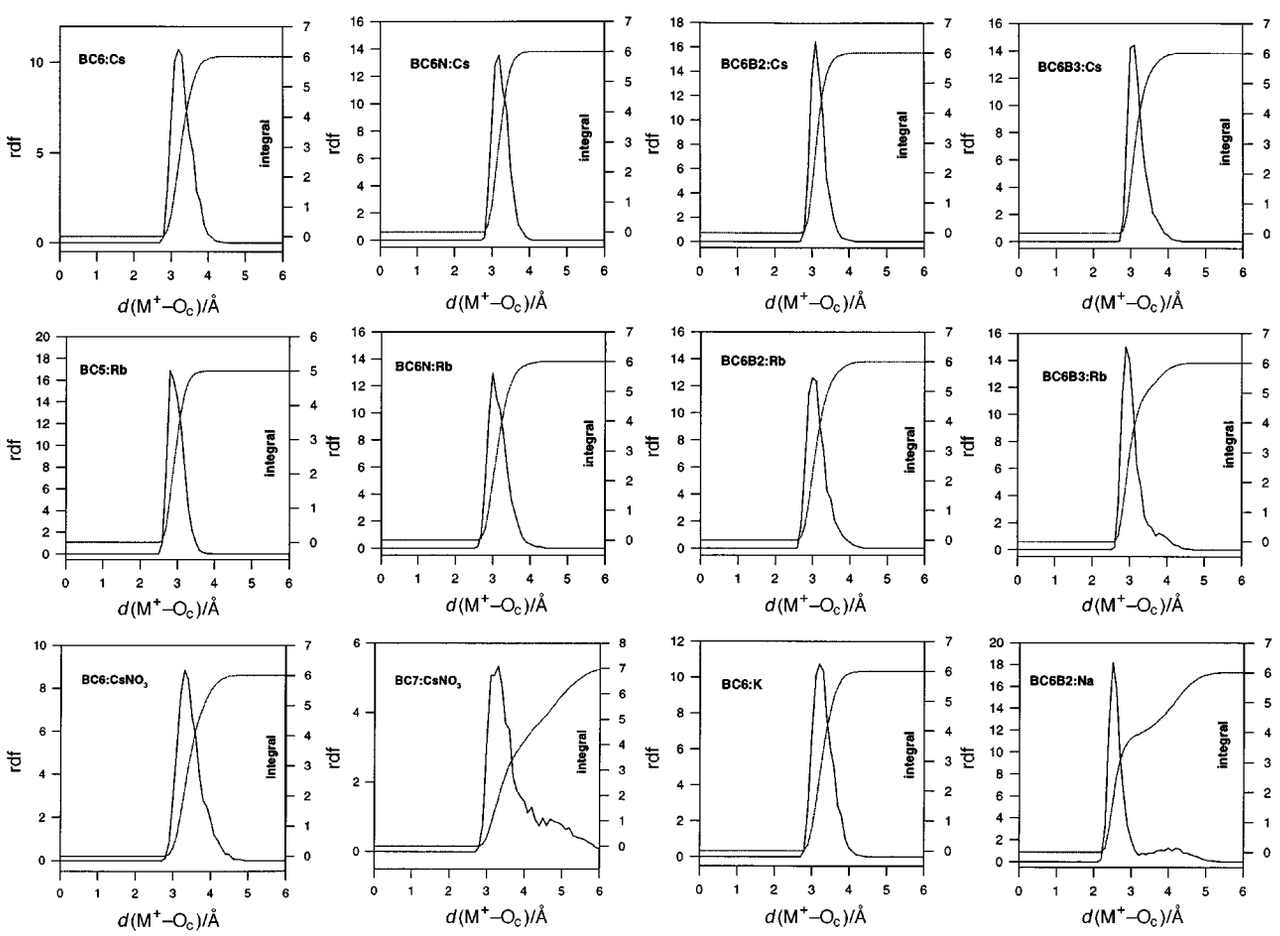

Fig. 2 Radial distribution function $rdfO_C$ of the crown oxygen atoms around the cation during 500 ps of MD in vacuum at 300 K.

which tends to draw the cations out of the mean plane of the crown ether loop and provides evidence of the existence of various metastable configurations. Simulations with $CsNO_3$ and calixcrown-6 ligands (Fig. 4) showed a slight discrimination between **BC6B3**, **BC6B2** and **BC6N**, since the best fit was then obtained with **BC6B2** (on the rdf curve, the peak maximum is set at 3.2 Å for **BC6B2** (narrow) and **BC6B3** (enlarged), to be compared to 3.3 Å for **BC6N** and **BC6**), but structures are

Table 2 Cation hydration in complexes with calix[4]arene-bis-crowns

	nO_w [a]				
	BC5	**BC6B3**	**BC6B2**	**BC6N**	**BC6**
Cs^+	1.0	1.0	1.5	0.8	1.1
Rb^+	0.5	1.3	1.7	1.0	1.0
K^+	1.0	0	1.3	1.0	3.0
Na^+	1.0	0	0	*b*	0

[a] Number of water oxygen atoms in the first hydration shell of the cation complexed by the calixcrown during the MD run in a water box (rdf collected from 15 to 100 ps of MD run excepted for **BC6B3**–Cs^+ (hydration at 40 ps) and **BC6**–K^+ (stabilization at 3.0 O_w since 60 ps, average of 2.0 O_w from 15 to 100 ps)). [b] Decomplexed.

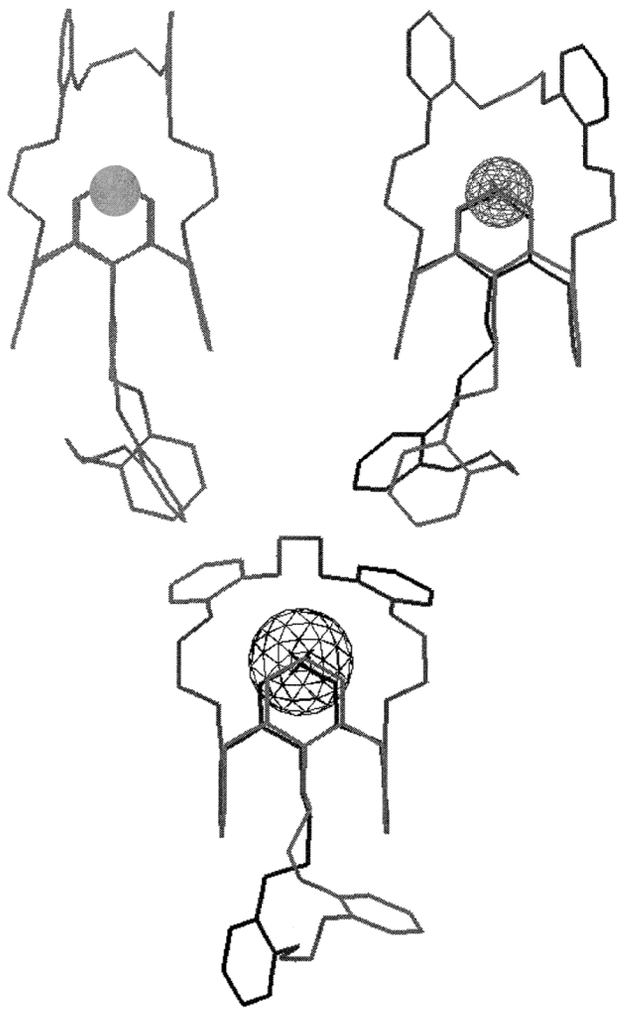

Fig. 3 Minimized **BC6B2**–Na^+, K^+ and Cs^+ structures in a vacuum (H atoms not represented).

rather close to those obtained without counter-ion for these ligands. On the contrary, structures simulated in a vacuum with $NaNO_3$ give rise to a different location of the sodium ion: whatever the calixarene, this small cation is shifted to the upper part of the crown, interacting with the nitrate and four oxygen atoms of the crown (Fig. 5). This location leaves enough room for a water molecule in the crown. In a previous study, taking advantage of a **BC6**$(NaNO_3)_2(H_2O)_2$ X-ray structure, we have described how sodium complexation was probably favored by one of the water molecules of the cation hydration shell, leading to a partial dehydration of the sodium upon complexation.[24] This behavior has been checked on several MD simulations with **BC6**, and is independent of the charge sets tested. The presence of hydrophobic aryl groups on the complexation site is a handicap for the action of the water molecule. Indeed,

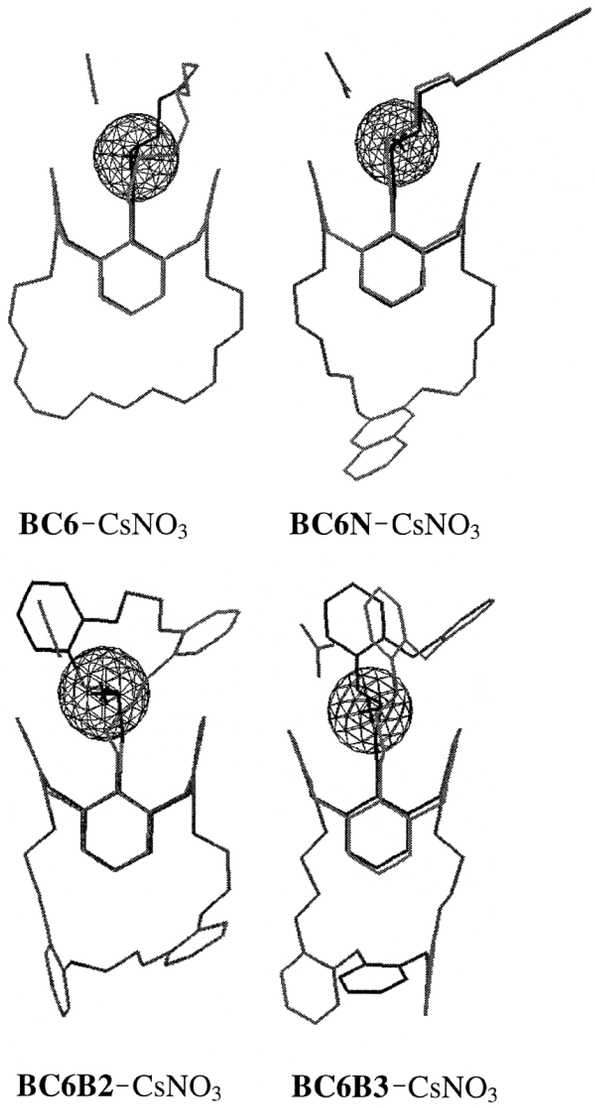

Fig. 4 Minimized $CsNO_3$ complexes with calix[4]arene-bis-crown-6 *in vacuo.* (H atoms not represented).

total decomplexation of sodium is always observed during MD simulations in water on binuclear sodium nitrate complexes with **BC6B3**, **BC6B2** and **BC6N**. The situation is less clear starting with mononuclear $NaNO_3$ complexes, since, in one simulation with **BC6B2**, such a hydration occurred, although with **BC6B3** the simulation was stopped at 150 ps of MD run without any contact between the cation and the water phase.

So if complete dehydration of the sodium cation is energetically at a disadvantage (see free energy calculations in water), the Na^+ complexation with partial dehydration appears to be possible but obstructed by the presence of hydrophobic benzo groups on the crown. The decrease of affinity towards sodium in this calixarene family must be related to this hydrophobic unfavorable environment more than to worse Na^+–calixarene complementarity.

The crown size can be represented by the $\langle d(C–O_C)\rangle$ parameter, mean distance of the oxygen atoms of the crown to their mass center. This value was calculated on a MD sampling of at least 500 ps in a vacuum, for both crowns in the free ligand, and, for the empty crown, in the mononuclear alkali complexes (Table 1). The free calixarenes need different sampling times at 300 K to obtain the convergence of $\langle d(C–O_C)\rangle$ towards the same value for both crowns. Indeed, 500 ps at 300 K are sufficient for **BC5**, **BC6B3** and **BC6B2**, 1 ns at 300 K is needed for **BC6**, but convergence was not obtained for **BC6N** at 4 ns of MD run at 300 K, and one more sampling of 1 ns at 500 K was necessary to obtain the value. This difficulty in sampling **BC6N** crowns

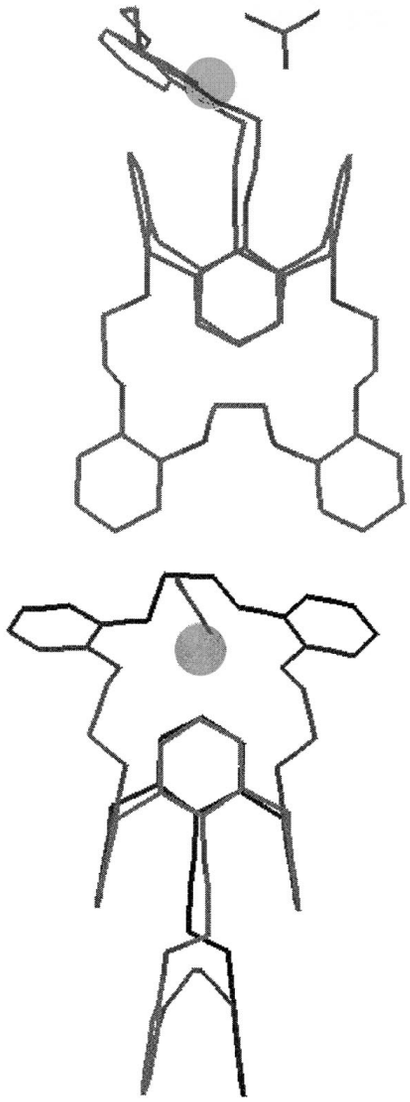

Fig. 5 Minimized **BC6B2**–$NaNO_3$ structure *in vacuo* (orthogonal views, H atoms not represented).

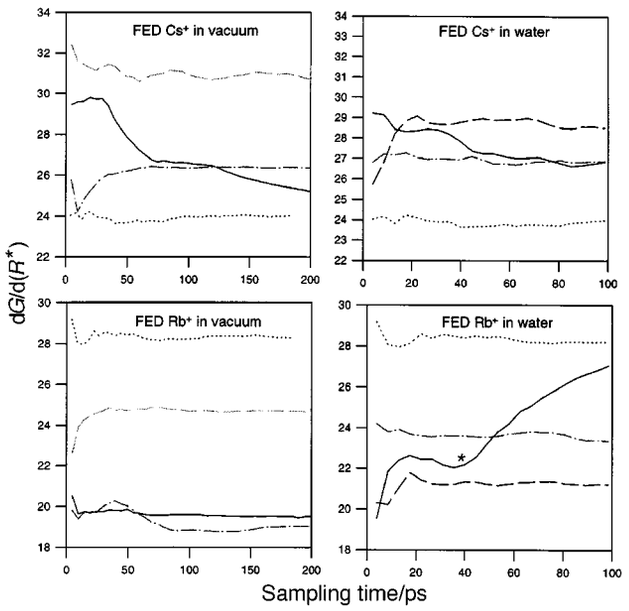

Fig. 6 Time evolution of the free energy derivative with respect to the van der Waals parameter R^* for Cs^+ and Rb^+ cations complexed in the benzocrown calixarenes (simulations *in vacuo* and in water). (——) **BC6B2** complex, (---) **BC6B3** complex, (–•–) **BC6N** complex, (····) free cation in water, * partial decomplexation.

has been previously observed with our former charge set,[23] and appears to be a property of **BC6N**, compared to other calixcrowns: the rigidification of the top of the crown increases the energetic barrier to sample the free dihedrals.

When one of the crowns is complexed, an influence of the complexed crown on the organization of the free crown is observed for **BC6B3**, **BC6N** and **BC6**, whose $\langle d(C–O_C)\rangle$ and associated fluctuation decrease. Finally, the size of the complexed crown, which changes with respect to the cation and the presence of the counter-ion, is generally smaller than the size of the free crown due to the converging position of the oxygen atoms towards the cation.

Thus, our overall conclusions from the present MD simulations are that *all the calixcrown-6 ligands, especially those bearing aromatic substituents, show a good complementarity for* Cs^+. The adjunction of those aromatic substituents decreases the crown size and ameliorates the affinity for Rb^+, although it remains far from the perfect fit obtained with **BC5**. But *none of the ligands studied shows a significant complementarity for* Na^+. Relative discrimination of these calix[4]arene-crown-6 ligands towards Na^+ complexation seems mostly driven by the possibility of solvation of the cation in the complex.

Free energy calculations

The three free energy derivatives were calculated on alkali-metal cations in calixcrown complexes, as a function of sampling time for 200 ps in a vacuum and 100 ps in water. Their convergence is slower for the complex cations than for their hydrated forms (see Experimental section). The van der Waals parameters of Rb^+ and Cs^+ converge very slowly and, in these cases, it seems necessary to sample for at least 50 ps to achieve full convergence whether in a vacuum or in water (Fig. 6). Some FEDs did not converge due either to partial decomplexation (**BC6B2**–Rb^+ in water, where, after 45 ps, the cation is partially out of the crown, bound by one water molecule within the crown) or to great sensitivity to changes in OCCO dihedral angles (**BC6B2**–Cs^+ in a vacuum). The protocol 11(2 + 50) was then chosen for mutations in a vacuum but the necessity to keep reasonable calculation times led us to choose as the standard for mutations in water, the protocol 11(2 + 20). It can be argued that this sampling is sufficient, as it has already been shown, here and elsewhere,[45] that full convergence of the free energy derivatives is not necessary to gain satisfactorily accurate results for the free energy calculations for cation mutation. Nevertheless, the sampling time evolution of the FEDs with respect to the cation parameters shows that, as in the case of **BC6B2**, it will be difficult to get reliable quantitative results for the mutation of larger cations in either a vacuum or water. These FED calculations do not allow us to conclude which calixcrown-6 has the best affinity towards Cs^+ or Rb^+, but, in any case, the optimum ion for these macrocycles has a size between Rb^+ and Cs^+, as it has been previously found that the optimum cation size for 18-crown-6 is slightly smaller than K^+.[46]

Selectivity calculations were performed with the thermodynamic cycle method where the intrinsic preference of a ligand for a cation is indicated by the value of $\Delta G_{4\ vac}$. Values for the present systems were calculated with the protocol 11(2 + 50) and show the usual preference for the smallest ions ($\Delta G_{4\ vac} > 0$, Table 3). The difference $\Delta G_{3\ wat} - \Delta G_{4\ vac}$ can give an indication of possible selectivity in extraction from an aqueous phase to an apolar organic phase, if there are no major differences in cation solvation energy in the complexes, as has been found in simulations of **BC6** alkali-metal ion complexes in chloroform.[30,33] The predicted selectivity for **BC6**, **BC6N** and **BC6B2** is much the same, with $Cs^+ > Rb^+ > K^+ > Na^+$, though **BC6B2** would appear to offer least discrimination. For **BC6B3**, the

Table 3 $\Delta G_{4\ vac}$[a] calculated from MD/TI *in vacuo*, and $\Delta G_{3\ calc}$ calculated from MD/TI in water

		$Na^+ \rightarrow K^+$	$K^+ \rightarrow Rb^+$	$Rb^+ \rightarrow Cs^+$
$\Delta G_{4\ vac}$/kJ mol^{-1}	**BC6**	34.5(1.0)	14.0(0.5)	26.3(6)
	BC6N	31.8(1.3)	13.7(0)	28.0(2)
	BC6B2	38.4(5)	15.2(0)	30.2(8)
	BC6B3	37.1(1)	18.1(0)	**35.7(0)**[b]
	BC5	38.5(5)	20.4(1)	**44.0(0)**[b]
$\Delta G_{3\ calc}$/kJ mol^{-1}		73.4(1)	22.7(0)	32.8(1)

[a] Averages of two independent simulations. [b] In bold characters, selectivity for rubidium ($\Delta G_{3\ calc} - \Delta G_{4\ vac} < 0$).

selectivity is predicted, on the basis of the mutation criterion, to change such that there is the greatest affinity for Rb^+ (as is the case, though more markedly, for **BC5**) but this result is inconsistent with estimates of the host–guest complementarity which indicate that the preference still should be for Cs^+.

Calculation of $\Delta G_{4\ wat}$ in water could not be fully achieved due to cation decomplexation during most of the mutations. One could notice that $\Delta G_{4\ wat}$ values between Rb^+ and Cs^+ were close to $\Delta G_{4\ vac}$ even when these cations were hydrated in the calixarene. A difference of about 4 kJ mol^{-1} between $\Delta G_{4\ wat}$ and $\Delta G_{4\ vac}$ was found for mutations between K^+ and Rb^+, but the $\Delta G_{4\ wat}$ values most sensitive to the hydration of the complex were found for the mutations between Na^+ and K^+, ranging from 40 kJ mol^{-1} for the non-hydrated ion (close to $\Delta G_{4\ vac}$ value) to about 76 kJ mol^{-1} when the cation is in contact with a water molecule, leading to a strong decrease in calculated selectivity with respect to Na^+. These simulations confirm that the hydration of the sodium ion in the calixcrown-6 is a key feature of selectivity between Na^+ and other alkali cations.

Experimental investigations

Synthesis of BC6B2

The synthesis of the new ligand **BC6B2** is presented in Scheme 1. It follows procedures which are now well established from the preparation of a number of calixcrowns.[16] The synthesis is remarkable in all cases in that the formation of two macrocyclic, polyether units on one calixarene base occurs in acceptable yields without the need for special reaction conditions such as the use of high dilution. It is possible that cation template effects are of some influence in the reactions but since the reaction mixture is at all times heterogeneous, it is extremely difficult to be sure of any mechanistic details.

Doubly crowned calix[4]arene **BC6B2** was fully characterized by ^{1}H-NMR, FAB spectrometry and elemental analysis. The 1,3-alternate conformation was deduced from its ^{1}H-NMR spectra, which showed singlets at 3.74 ppm for the Ar–CH_2–Ar methylene protons in the macrorings of **BC6B2**. The simplicity of the polyether chain methylene resonances in particular indicates that the chains must be conformationally mobile on the NMR timescale.

Crystal structures of BC6B2·CH_3NO_2 1 and $Cs_2(NO_3)_2$BC6B2·$CHCl_3$·H_2O 2

An ORTEPII view of the molecular unit of **1**, which does not possess any symmetry element, is given in Fig. 7. We have recently reported the crystal structures of solvent adducts of **BC6** and **BC6N**.[22,23] The presence of complexed solvents has been shown to have an influence on the crown conformation:[23] polar solvents such as acetonitrile and nitromethane were shown to interact with the crown ether oxygen atoms *via* weak C–H···O hydrogen bonds with their methyl group pointing towards the crown center. The present structure illustrates by itself such an effect since a nitromethane molecule is associated with one of the two crowns (corresponding to O1–O6) and not

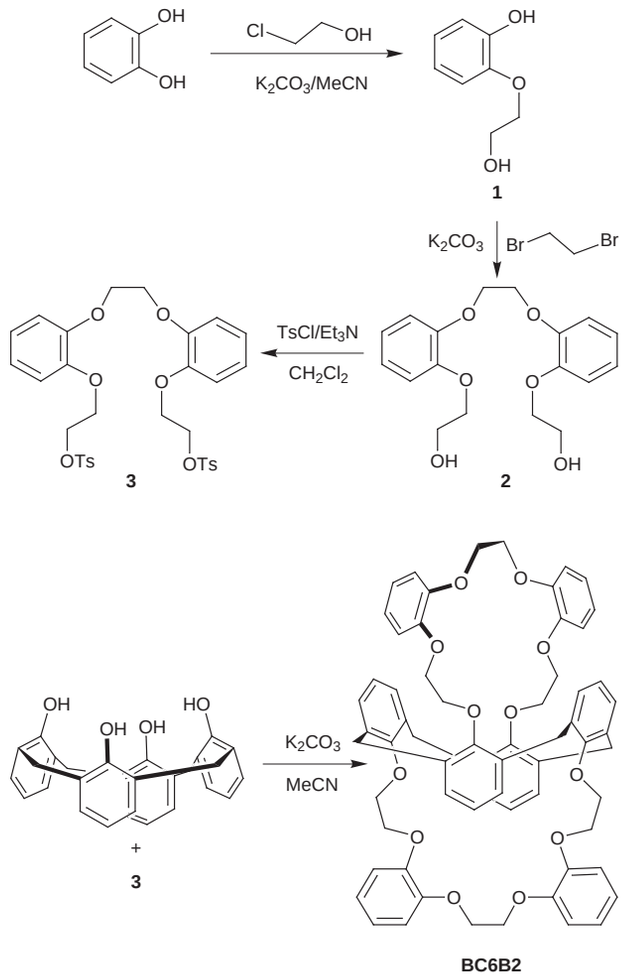

Scheme 1

with the other one (O7–O12). The location of this solvent molecule is comparable to that in the **BC6** and **BC6N** cases: the C(methyl)···O(ether) distances range from 3.16(1) to 3.49(1) (mean value 3.4(1)) Å and the C(methyl) atom is 1.29(1) Å from the mean plane defined by the six oxygen atoms O1–O6 (defined within ±0.305(6) Å). The crown conformations cannot be directly compared to those of **BC6** and **BC6N** since two torsion O–C–C–O angles are constrained to the zero value by the phenyl rings. These conformations can be described by the sequence of O–C–C–O torsion angles, which is $g^-0g^+0g^+$ for O1–O6 and $a0g^-0a$ for O7–O12 (g = *gauche* angle, a = *anti* angle). Moreover, not all the C–O–C–C torsion angles are *anti* ones: some of them are *gauche* angles or intermediate values: the departure from 180° is particularly evident near O8 and O11 whose lone pairs point outwards. On the contrary, the oxygen atoms' lone pairs in the crown, including the solvent molecule, are all directed towards the crown centre as in the caesium complexes.[20–23]

The molecular unit of **2** is shown in Fig. 8. The two caesium ions are included in the crown ether moieties, as in the complexes described previously.[20–23] A particular feature of the present structure concerns the counter-ions. Whereas in the previous structures, the nitrate ions were always bonded to the caesium ion in a bidentate mode (with the exception of a monodentate one[21]), one of the nitrate ions in the present case is not bonded and the other one bridges the caesium ions of two neighboring molecules (bidentate for one, monodentate for the other) thus giving rise to polymeric infinite chains. The formation of dimers has already been observed with thiocyanate counter-ions.[20] The caesium ions are bonded to the six oxygen atoms of each crown, with distances ranging from 3.094(3) to 3.366(3) (mean value 3.26(11)) Å for Cs1 and from 2.995(4) to

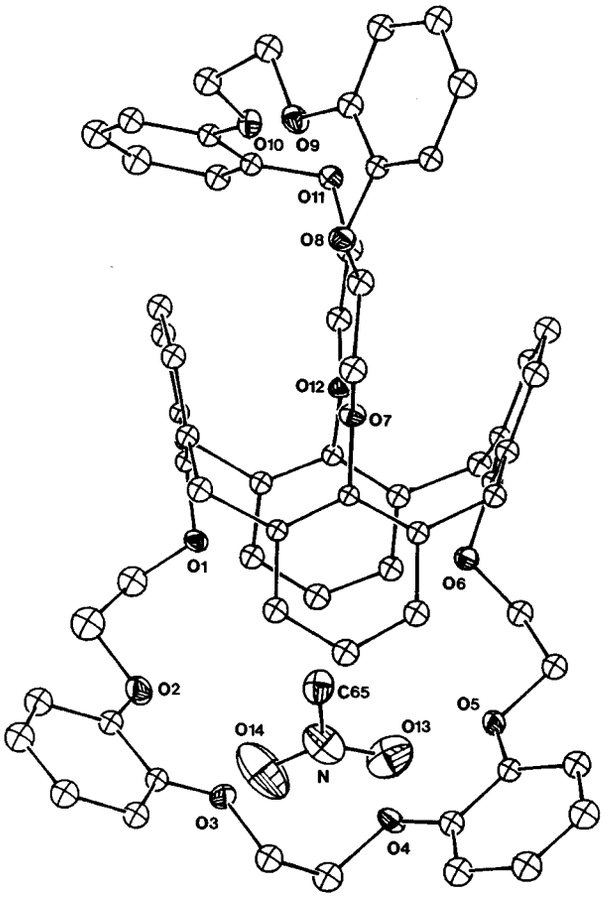

Fig. 7 X-Ray crystal structure of **BC6B2**·CH_3NO_2 **1**. Hydrogen atoms omitted for clarity. Shorter intermolecular contacts (Å): C65···O1 3.38(1), C65···O2 3.46(1), C65···O3 3.49(1), C65···O4 3.16(1), C65···O5 3.36(1), C65···O6 3.48(1).

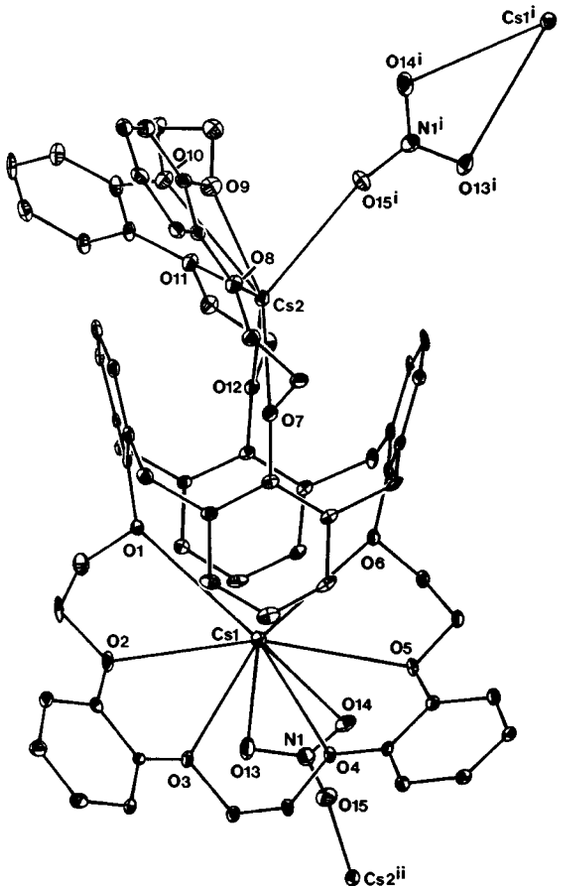

Fig. 8 X-Ray crystal structure of $Cs_2(NO_3)_2$**BC6B2**·$CHCl_3$·H_2O **2**. Hydrogen atoms, non-coordinating nitrate ion and solvent molecules omitted for clarity. Symmetry operations: i = 1/2 − *x*, *y* − 1/2, 3/2 − *z*; ii = 1/2 − *x*, 1/2 + *y*, 3/2 − *z*. Selected bond lengths (Å): Cs1–O1 3.366(3), Cs1–O2 3.305(4), Cs1–O3 3.094(3), Cs1–O4 3.299(3), Cs1–O5 3.336(3), Cs1–O6 3.137(3), Cs1–O13 3.363(4), Cs1–O14 3.208(4), Cs1···C47 3.600(5), Cs1···C48 3.367(5), Cs1···C49 3.602(5), Cs1···C61 3.695(5), Cs1···C62 3.416(5), Cs1···C63 3.619(5), Cs2–O7 3.229(3), Cs2–O8 3.297(4), Cs2–O9 2.995(4), Cs2–O10 3.278(4), Cs2–O11 3.349(4), Cs2–O12 3.088(3), Cs2–O15^{i} 3.186(4), Cs2···C39 3.627(5), Cs2···C40 3.436(5), Cs2···C41 3.615(5), Cs2···C54 3.680(5), Cs2···C55 3.458(5), Cs2···C56 3.679(5).

3.349(4) (mean value 3.21(14)) Å for Cs2. These values are in agreement with those in the complexes previously described; they are slightly lower than those determined for **BC6** complexes with bidentate nitrate ions (3.4(1) Å), and closer to those obtained with a monodentate nitrate ion (3.18(6) Å) or in the case of **BC6B** or **BC6N** complexes (3.3(2) Å). This is in qualitative agreement with the crown sizes deduced from molecular modelling (see Table 1 above). The distances between caesium ions and the oxygen atoms' mean planes are 0.83(2) and 0.72(2) Å for Cs1 and Cs2 respectively. Both distances are in the usual range; however, the caesium ion is bonded to only one nitrate oxygen atom, hence possesses a less bulky counter-ion, and thus seems to be slightly nearer to the crown. Due to the peculiar binding mode of the counter-ion, the distances between caesium ions and the nitrate oxygen atoms lie a little above the usual range: 3.363(4) and 3.208(4) Å for Cs1, 3.186(4) Å for Cs2, to be compared to mean values of 3.08(6)–3.2(1) Å in the previous cases (3.15(1) Å for the monodentate nitrate ion). The monodentate bond length appears slightly shorter than the bidentate means. The shorter Cs···C distances, as usual, are with the three terminal atoms of the phenolic rings, with mean values of 3.5(1) Å for Cs1, 3.6(1) Å for Cs2 (3.5(2) to 3.6(2) Å in the previous cases). The conformations of the two crowns are identical: the O–C–C–O angles give the sequence $g^{-}0g^{-}0g^{+}$, analogous to the one observed in the solvent-containing crown in **1**, and two C–O–C–C angles deviate from the ideal *anti* value (81 and 94°). Once more, it is found that a caesium ion or a solvent molecule (nitromethane or acetonitrile) organizes the crowns in very similar ways, whereas empty crowns, due to their high flexibility, may display completely different conformations.[23] The conformation observed here is roughly the same as those found in the caesium and potassium complexes of the mono-crown derivative: $g^{-}0a0g^{+}$, with $a = 29°$ for Cs^+ and $g^{-}0g^{+}0g^{+}$ for K^+ and, in both cases, deviations of some C–O–C–C angles from the ideal value.[43] The crystal structures of the complexes with the unsubstituted crown derivative have already shown that caesium and potassium ions induce the same crown conformation.[24]

Complexation studies

Preliminary studies of alkali picrate complexation by **BC6B2** were monitored with ^{1}H-NMR. After a reaction period of approximately 72 hours between solid alkali metal picrates (Li^+, Na^+, K^+, Rb^+ and Cs^+) and a chloroform solution of **BC6B2**, the ratios of metal to ligand in solution, as estimated from integration of the picrate proton resonances *versus* those for the methylenic protons Ar–CH_2–Ar, were 0.4 : 1 (Li^+), 0.1 : 1 (Na^+), 0.4 : 1 (K^+), 1.3 : 1 (Rb^+), and 1.0 : 1 (Cs^+). These ratios must be determined partly by differences in the lattice energy of the solid picrates as well as by differences in complex ion stability, and may possibly be affected by the fact that lithium and sodium picrates are hydrated, whereas those of potassium, rubidium and caesium are not, though no special care was taken to dry $CDCl_3$ used. All spectra in fact showed (weak) water resonances of similar intensity, but one can deduce from these values a preference for Rb^+ and Cs^+ over the other alkali metal ions.

Table 4 Interaction of alkali metal ions with **BC6B2**: percentage extraction E^a from water into dichloromethane; stability constants log β_{xy} [b] and thermodynamic parameters [c] in acetonitrile; association constants log K_a and position of the maximum absorption λ_{max} [d] of the separated ion pair in tetrahydrofuran, with, in parentheses, the shift *vs.* the position of the maximum absorption of the tight ion pair. (Mean values of $n \geq 2$ independent determinations, with the standard deviation on the mean, σ_{n-1})

	Li^+	Na^+	K^+	Rb^+	Cs^+
E	0.9 ± 0.2	0.9 ± 0.1	11.3 ± 0.1	40.4 ± 0.3	56.0 ± 0.1
Log β_{11}	2.18 ± 0.03	≤1	5.22 ± 0.05	5.5 ± 0.2	6.3 ± 0.1
$-\Delta G_{11}$	—	≤5.70	29.8 ± 0.3	31 ± 1	35.9 ± 0.6
$-\Delta H_{11}$	—	[e]	10.7 ± 0.7	22.7 ± 0.2	29 ± 1
$T\Delta S_{11}$	—	—	19 ± 1	8 ± 1	7 ± 2
Log β_{21}	—	—	8.05 ± 0.07	9.4 ± 0.1	10.1 ± 0.2
$-\Delta G_{21}$	—	—	45.9 ± 0.4	53.6 ± 0.6	58 ± 1
$-\Delta H_{21}$	—	—	23.8 ± 0.6	46.1 ± 0.5	54 ± 3
$T\Delta S_{21}$	—	—	22 ± 1	8 ± 1	4 ± 4
Log K_a	—	[f]	4.0 ± 0.1	4.91 ± 0.09	5.75 ± 0.04
$\lambda_{max}(\Delta\lambda_{max})$	—	—	375(17)	378(19)	377(16)

[a] $T = 20$ °C. [b] $T = 25$ °C, $I = 0.01$ M (Et_4NClO_4); corresponding to the general equilibrium: $xM^+ + yL \rightleftharpoons M_xL_y^{x+}$. [c] $T = 25$ °C, ΔG, ΔH and $T\Delta S$ in kJ mol^{-1}. [d] λ_{max} in nm. [e] Not measurable. [f] No spectral changes observed.

Extraction data (Table 4) show that with **BC6B2**, as with all the bis-crown-6 derivatives previously studied,[18] there is an increase in percentage extraction (E) along the alkali metal series. It can be noted that the extraction level of the larger cations is less affected by the substitution of the crown linkage than the smaller ones. For instance, the extraction of Cs^+ is only slightly decreased when one and two benzo groups are attached to the crown moieties, whereas the extraction of Na^+ is strongly decreased. These variations lead to an increase in the Cs^+/Na^+ extraction selectivity $S = E_{Cs^+}/E_{Na^+}$ from 14 to 29 and 62, for **BC6**, **BC6B** and **BC6B2** respectively.

Complexation studies of **BC6B2** in a homogeneous medium were limited because of the low solubility of this ligand. However stability constants could be determined in acetonitrile and were compared to those obtained previously for **BC6**, **BC6B** and **BC6N**.[18] These results had shown that the substitution of the crown-6 parts of **BC6** by a 1,2-phenylene or a naphtho group led to practically no change in the complexing properties towards the large cations K^+, Rb^+ and Cs^+, and a small but systematic decrease of the complex stability with the smaller cations Li^+ and Na^+. This led, as already observed in extraction, to an increase of the Cs^+/Na^+ selectivity from **BC6** to **BC6B** and **BC6N**,[18] which has been interpreted in terms of loss of flexibility of the crown chain, the substituents rigidifying the crown and preventing optimal interactions between the binding sites and the smaller cations. The introduction of a second 1,2-phenylene group like in **BC6B2** leads to important modifications in both the nature and the stability of the complexes formed. With K^+, Rb^+ and Cs^+, the experimental spectrophotometric data present firstly a series of spectra passing through an isosbestic point until $C_M/C_L \approx 1$ (for Cs^+ and Rb^+) and $C_M/C_L \approx 2$ (for K^+), followed by a second set of spectra with increasing intensities for higher values of C_M/C_L. Fig. 9 illustrates the case of Cs^+. These spectral changes clearly show the presence of three distinct absorbing species (including the ligand) and have been interpreted by the formation of a binuclear species as well as the mononuclear complex (Table 4). The binuclear complex of Cs^+ has been isolated in the solid state and its structure is reported in this paper. The formation of binuclear complexes had already been shown with Cs^+ in solution by NMR [21] and in the solid state for the three ligands **BC6**, **BC6B** and **BC6N**.[14,20,21,23] Complexation of Li^+ leads to a small but regular decrease in the intensities of the spectrum of the ligand, as was previously observed with the other bis-crown-6 derivatives and all alkali metal ions,[18] indicating the formation of a mononuclear complex only. With Na^+, no spectral changes could be observed even in the presence of a large excess of metal ion.

The stability of the 1:1 complexes of **BC6B2** roughly confirms the trends observed in extraction, *i.e.* an affinity for the large cations K^+, Rb^+ and Cs^+.[18] The introduction of two 1,2-phenylene groups on each crown unit of **BC6** results in a decrease in the stability of the sodium complex and an increase in the stability of the complexes with the larger cations K^+, Rb^+ and Cs^+ (*e.g.* $\Delta\log\beta_{11} = 1.4$ in the case of Cs^+), whereas the stability of the Li^+ complex surprisingly remains almost the same. The Cs^+/Na^+ selectivity increases from **BC6** to **BC6B**, **BC6N** and **BC6B2**, although the selectivity of the latter ligand ($S = \beta_{Cs^+}/\beta_{Na^+} \geq 2 \times 10^5$) cannot be strictly evaluated because of the very weak stability of the Na^+ complex, which could only be estimated to be lower than 1 log unit.

The substitution of the crown parts of bis-crown-6 deriv-

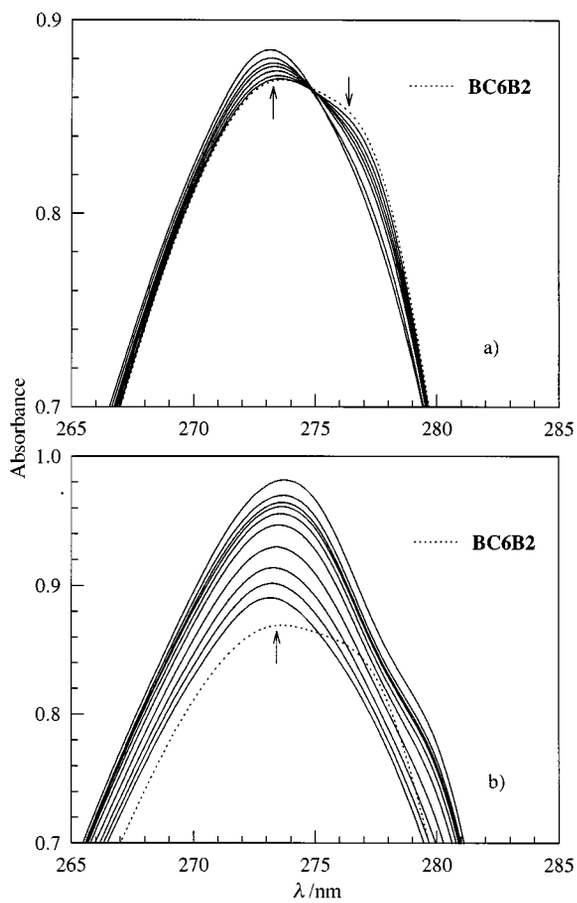

Fig. 9 Changes in the UV absorption spectrum of **BC6B2** ($C_L = 8.2 \times 10^{-5}$ M) upon addition of $CsNO_3$ in acetonitrile: a) $0 \leq C_M/C_L \leq 0.9$ b) $1.1 \leq C_M/C_L \leq 14.3$; spectrophotometric cells of 1 cm pathlength.

atives by one aryl group had been shown to lead to important changes in the stabilization of the complexes.[18] In particular, it induces a strong decrease in the enthalpy of complexation ($-\Delta H_{11}$) and a strong increase in the corresponding entropy ($T\Delta S_{11}$). This had been interpreted by the rigidification of the molecule, which weakens the interactions between the binding sites and the cations, and counteracts the loss of degrees of freedom upon complexation. The substitution of the crown moieties by two 1,2-phenylene groups also leads to some changes in the stabilization of the complexes. As seen from the calorimetric data in Table 4, the stabilization of the K^+, Rb^+ and Cs^+ complexes of **BC6B2** in acetonitrile is both enthalpy and entropy driven ($-\Delta H_{11} > 0$ and $T\Delta S_{11} > 0$). This contrasts with the stabilization of their homologs with **BC6** which was mostly enthalpy controlled.[18] However, in agreement with what was observed with **BC6**, $-\Delta H_{11}$ values decrease in the series from Cs^+, to Rb^+ and K^+, whereas $T\Delta S_c$ values increase. As for the unsubstituted ligand, the enthalpy variations can be interpreted in terms of size adequacy between the cation and the crown loop, the crown size being too large to allow efficient interaction with the smaller cations. The entropy changes are related to the stronger desolvation of these cations upon complexation and to a smaller loss of conformational freedom of the complexed crown moiety.

The higher stability of **BC6B2** complexes over **BC6** ones is entirely due to the more favourable entropy terms (Table 4). This can be explained by the greater rigidity of **BC6B2** and its smaller loss of freedom upon complexation. The rigidity is also reflected in the enthalpy changes. Although the $-\Delta H_{11}$ value for the complexation of Cs^+, whose size is well adapted to the crown, is similar to that observed with **BC6**, it is lower with the smaller and less suited Rb^+ and K^+ cations, indicating the difficulty encountered by the di-substituted crown part in accommodating these cations.

Comparison between **BC6B2** complexes and their homologs with **BC6B** and **BC6N** bearing only one aryl group is less straightforward (Fig. 10). Stabilization of **BC6B** and **BC6N** complexes has been shown to be mostly entropy driven ($-\Delta H_{11} > 0$ and $T\Delta S_{11} > 0$, $T\Delta S_{11}$ being dominant).[18] The extra stability of Rb^+ and Cs^+ complexes with **BC6B2** is now due to a more favorable enthalpy term overcoming a less favorable entropy term. Different factors may account for this behavior: the higher $-\Delta H_{11}$ value may reflect a better preorganization or complementarity of the bis(1,2-phenylene)-crown derivative as well as the possibility of strong π-interactions with the cation through the two benzo rings.[46] The lower solvation of the di-substituted ligand may also be associated with a higher enthalpy contribution. All these effects must be predominant over the effect of decreased basicity of the oxygen donor sites due to the presence of the benzo rings.[47] The smaller entropy term is consistent with the lower solvation of the ligand and its lower rigidity with respect to **BC6B** and **BC6N**.

The binuclear complexes found with **BC6B2** and the three cations K^+, Rb^+ and Cs^+ are less stable than the corresponding mononuclear complexes. The lack of positive cooperative effect in their formation is essentially due to unfavorable entropy terms. The enthalpy of complexation corresponding to the stepwise formation of the binuclear complex $\Delta H_2 = \Delta H_{21} - \Delta H_{11}$ and the corresponding entropy terms $T\Delta S_2 = T\Delta S_{21} - T\Delta S_{11}$ can be calculated from the overall values given in Table 4. It can be seen that, whereas $-\Delta H_2$ and $-\Delta H_{11}$ values are of the same order of magnitude, $T\Delta S_2$ values are very low when compared to $T\Delta S_{11}$. For instance, $T\Delta S_2$ is found to be 3 kJ mol^{-1} instead of 19 kJ mol^{-1} for $T\Delta S_{11}$, for the K^+ complex. This may show a loss of freedom of the system upon complexation of the second cation, resulting from its organization and rigidification.

The separation of the tight ion pairs formed by alkali picrates in a medium of low relative permittivity gives another picture of the complexing ability of a given ligand. The association

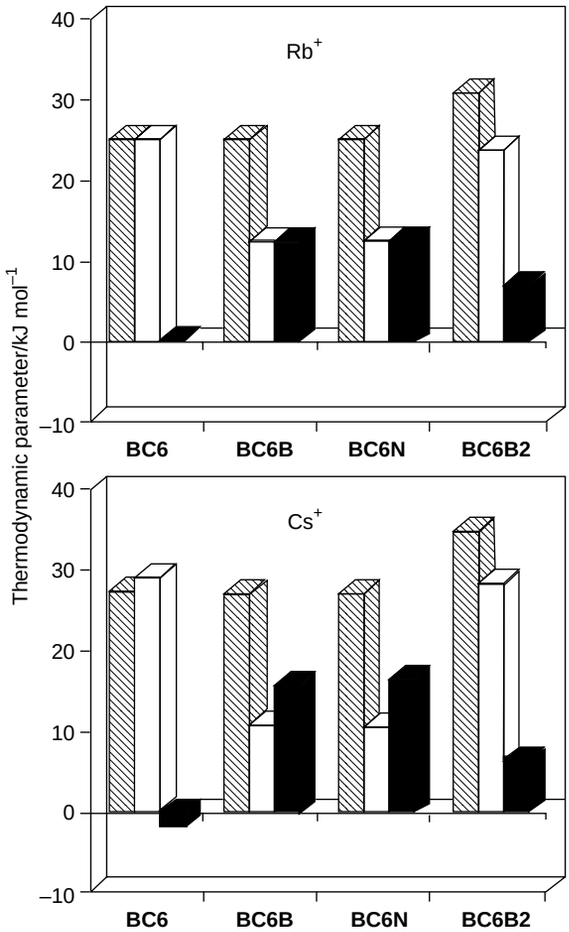

Fig. 10 Thermodynamic parameters for the complexation of Rb^+ and Cs^+ by calix[4]arene-bis-crown-6 in acetonitrile. ▨ ΔG_{11}, □ ΔH_{11}, ■ $T\Delta S_{11}$.

constants log K_a corresponding to the formation of the separated ion pairs from the tight ion pairs are also given in Table 4. These values do not display any systematic trend. The introduction of two 1,2-phenylene groups on the crown-6 parts can lead to either a decrease in log K_a as in the case of Rb^+, to an increase as in the case of Cs^+ or to practically no change as for K^+. However, the optical shifts, $\Delta\lambda$, experienced by the maximum absorption of the tight ion pair seems to be more informative: they are higher for Rb^+ and Cs^+ with **BC6B2** than with the other ligands.[48] In this case, the maximum absorption of the separated ion pair approaches the value of 380 nm, characteristic of the fully separated ion pair, suggesting a better shielding of these cations by **BC6B2** than by the other bis-crown-6 derivatives.

Discussion

In this study, there is an overall agreement between observations from MD simulations in a vacuum about crown size, crown rigidity, host–guest complementarity, and experimental data for the bigger cations. **BC6** appears too large for Cs^+, but flexible enough to optimize interactions on condition of a slight energetic loss in the entropic term upon complexation. The rigidification occurring in the top of the crown of **BC6N** decreases dramatically the flexibility of the crown, which is still too large, but is now unable to fit the cation well, which causes the loss in the enthalpic term. On the contrary, the gain in the entropic term shows a good preorganization of the crown due to the loss of flexibility and probably (but not illustrated in simulations) a weak solvation of the crown before complexation.

The **BC6B2**–Cs^+ complex is comparable to **BC6**–Cs^+ for the

enthalpic term, which underlines the good size complementarity. The entropic term is intermediate, stabilizing the complex but to a lesser extent than **BC6N**, and shows that the actual rigidification of the crown depends more on the location of the aromatic spacers than on their number. Thus, one can expect for **BC6B3** the qualities of **BC6N** (maximum of rigidification and minimum of solvation) without its drawback (smaller crown size). Nevertheless, the tail observed on the $rdfO_C$ curves could be a signal of too much rigidification, leading to difficulties for the oxygen atoms in arranging around the cation. Moreover, the crown size could this time be too small, which would lead to a selectivity for rubidium instead of caesium, as suggested by mutation calculations. So, this compound could have the same behavior as **BC5**, which is selective for Rb^+ and K^+ in extraction experiments. Here, the prediction limits of our model are reached, as there remains a doubt on the real selectivity of this new calixarene which has not been evaluated yet.[49]

Complex solvation has been taken into account with MD simulations in water. This solvent can be supposed not to be convenient for the study of these highly hydrophobic ligands because, although the structures obtained through simulations in vacuum may be compared with those obtained by X-ray diffraction, the hydrophobicity of the ligands means that the structural and energetic results obtained from simulations in an aqueous phase cannot be directly compared with experimental data for extraction. Water is present at every step of the extraction process and incomplete dehydration of the cation during complexation can give rise to a hydrated complex ion product. Such species have been proposed in order to rationalize extraction isotherms for K^+, Rb^+ and Cs^+ complexes of calixcrowns.[50] No evidence was obtained for similar behavior involving Na^+ but in fact the crystal structure of the binuclear $NaNO_3$ complex of **BC6** obtained from undried salt and methanol–acetonitrile solution shows that a hydrated species can form.[24] The main problem involved in MD simulations in water is the impossibility of simulating alkali complexes with counter-ions, with the exception of sodium, due to the high dissociating power of this solvent. Nevertheless, MD results from simulations in an explicit water phase show the possible hydration in a facial position of bigger alkali cations not coordinated with a counter-ion, which had been confirmed by an X-ray structure of the $KClO_4$–H_2O complex of 1,3-alt-dioctyloxycalix[4]arene C6B2, a monocrown analogue of **BC6B2**, whose perchlorate anion is dissociated from potassium.[43] In the case of sodium ion, MD simulations with nitrate counter-ion suggest that the selectivity in the alkali series, unfavorable to sodium, is due to the difficulty of sodium complexation without co-complexation of a water molecule, which is in agreement with the meanings of mutation calculations. The greater Cs^+/Na^+ selectivity of calixcrown-6 bearing 1,2-benzo groups with respect to the unsubstituted one, is expected to arise from the difficulty of complexation of Na^+–H_2O species in a more hydrophobic complexation site.

Studies of homogeneous phase complexation have shown that the introduction of a 1,2-benzo spacer at the head of the crown link has little influence on the binding of Cs^+ but strongly diminishes the interaction with Na^+. This effect is also reflected in the results for extraction of the alkali-metal picrates by the calixcrown ligands into dichloromethane. Enhancement of the extraction of Cs^+ under some experimental conditions, where the aqueous phase contains nitric acid, must be attributed to factors not quantified within our simulations and is possibly related to the increase of extractant hydrophobicity and the presence of acid.[17,51] Indeed, extraction isotherms have highlighted the formation of cation–nitric acid complexes for Cs^+ and Na^+ with the monocrown 1,3-alt-diisopropoxycalix[4]arene-crown-6.[50] It is known, in fact, that the substitution of alkyl by aryl groups within an extractant can improve the efficiency of the extractant in acidic media, a good example being provided by the optimization of the carbamoylmethylphosphine oxide (CMPO) ligands used in the "TRUEX" process for the extraction of trivalent lanthanides and actinides from nitric acidic solutions,[52] explained either by a weaker solvation of aryl substituted extractants, which are weaker bases than alkyl substituted ones and compete less with nitric acid,[53] or by an increase of the donor properties of the phenyl group as the oxygen atom is electron-depleted by charge transfer to the cation.[54] Such properties are not in the scope of current molecular modelling studies and should be investigated through quantum mechanics.

Conclusion

Molecular modelling, based on force field methods, has been used as a suitable method to explain the experimental Cs^+/Na^+ selectivity of a family of 1,3-alt-calix[4]arene-bis-crown-6, using an appropriate choice of force field parameters, mainly point charges. Calculations for new ligands belonging to this family before their synthesis, and focusing on host–guest complementarity, have shown that their affinity towards alkali cations was comparable to those of known compounds, with a possible inversion of the Cs^+/Rb^+ selectivity for the tribenzocrown-6 derivative not yet tested. In fact, the newly tested dibenzocrown-6 presents an enhanced Cs^+/Na^+ selectivity due to a poorer affinity for sodium cation. This feature is not the result of complementarity differences, and has been interpreted by the greater difficulty for the sodium cation to be complexed without total dehydration in a more hydrophobic complexation site.

Experimental

Simulation protocols

All calculations were carried out on SGI workstations (INDIGO 2 R8000 or Origin 200 R10000) with the AMBER 4.1 software,[55] using as a force field, the all-atom parameters and the representation of the potential energy given in eqn. (1).[56]

$$E_{pot} = \sum_{bonds} K_r(r - r_{eq})^2 + \sum_{angles} K_\theta(\theta - \theta_{eq})^2 + \sum_{dihedrals} \frac{V_n}{2}(1 + \cos(n\varphi - \eta)) + \sum_{i<j}\left[\varepsilon_{ij}\left(\left(\frac{R^*}{R_{ij}}\right)^{12} - \left(\frac{R^*}{R_{ij}}\right)^{6}\right)\right] + \sum_{i<j}\left[\frac{q_i q_j}{\varepsilon R_{ij}}\right] + \sum_{H\text{-bonds}}\left[\varepsilon_{ij}\left(\left(\frac{R^*}{R_{ij}}\right)^{12} - \left(\frac{R^*}{R_{ij}}\right)^{10}\right)\right] \quad (1)$$

The calixarenes were model built on the graphic workstation with the InsightII software[57] from previous optimized structures then submitted to a first minimization without atomic charges with the presence of the caesium cation in one crown.

The atomic charges on the calixarene were calculated with the MNDO semiempirical method without geometry optimization. The calculation was performed on the whole calixarene and the crude point charges thus determined were then averaged for equivalent atoms and scaled up with a 1.26 scaling factor to allow a nice fit with 6-31G*/ESP values commonly used for crown-ether moieties.[42] These point charges take into account different conformational environments (average on the complexed and the empty crown conformations) and no artifact is introduced by cutting the calixarene cavity. When possible, charges on equivalent atoms were kept constant through the series, but some significant differences were found due to the presence of benzo substituents on the crown (Fig. 11).

The cation parameters came from Aqvist[38] and were adapted to the AMBER force field (TIP3P water model and periodic boundary conditions). The 1–4 non bonded contributions were scaled down by a factor of 0.5.

In a vacuum, the alkali complexes were submitted to minimization with 50 steepest descent iterations followed by 1950 con-

Table 5 Evolution of calculated ΔG_3 with respect to the protocol of cations mutation

ΔG_3/kJ mol^{-1}	Exp. (Aqvist)[38]	21(1 + 4)[a] 105 ps	11(5 + 5) 110 ps	11(2 + 20) 240 ps	11(20 + 20) 440 ps	11(2 + 40) 460 ps
$Na^+ \rightarrow K^+$	73.7	72.2	73.4	73.3	72.6	73.4
$Rb^+ \rightarrow Cs^+$	32.3	33.3	33.0	32.9	32.8	33.1

[a] 21(1 + 4): 21 windows ($\delta\lambda = 0.05$) with 1 ps of equilibration and 4 ps of data collection by MD at 300 K. 20 ps of MD correspond to about 1 CPU hour on the SG R8000 workstation.

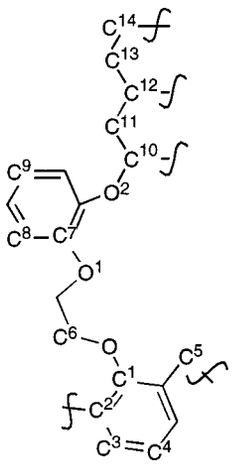

	BC6	BC6B2	BC6B3	BC6N
C1	0.157	0.150	0.150	0.150
C2	−0.140	−0.119	−0.119	−0.119
C3	−0.013	−0.020	−0.020	−0.020
H3	0.076	0.071	0.071	0.071
C4	−0.087	−0.082	−0.082	−0.082
H4	0.080	0.075	0.075	0.075
C5	−0.164	0.143	0.143	0.143
H5	0.000	0.001	0.001	0.001
O	−0.360	−0.346	−0.346	−0.346
C6	0.200	0.220	0.220	0.203
H6	0.000	0.000	0.000	0.000
O1	−0.400	−0.346	−0.346	−0.387
C7		0.120	0.103	
C8		−0.100	−0.083	
H8		0.087	0.091	
C9		−0.074	−0.071	
H9		0.080	0.085	
O2			−0.275	−0.346
C10			0.103	0.124
C11			−0.083	−0.089
H11			0.091	0.088
C12			−0.071	−0.042
H12			0.085	
C13				−0.051
H13				0.077
C14				−0.069
H14				0.077

Fig. 11 Point charges used in simulations.

jugate gradient iterations. Then MD simulations were performed at constant temperature (300 K) and energy for 500 ps with a 1.0 fs time step, the relative permittivity set at 1.0 and a 10 Å residue-based cut-off. One conformation was saved on each picosecond calculation and the trajectories, constituted of the collection of these conformations, were visualized on a graphics screen by the MD/DRAW software and analyzed by the MDS software.[58] The first ten picoseconds, corresponding to the system thermal equilibration, were not taken into account in the structural and energetic analysis and averages were calculated over 490 ps of MD.

In water, the molecular dynamics simulations used a time step of 2.0 fs, and a 12 Å cut-off. The SHAKE procedure was used to constrain bonds involving hydrogen atoms. We used PBC and an isothermal/isobaric ensemble of 300 K and 1 atm through coupling to temperature and pressure baths. All the starting structures were complexes minimized at the end of the MD run in a vacuum, and immersed in a TIP3P cubic box, removing water molecules within 2 Å of the solute (about 1200–1600 water molecules around the solute). These systems were energy minimized and submitted to at least 100 ps of molecular dynamics simulation (100 ps of MD in water took approximately 15 hours on one CPU of the R10000 computer).

Free energy calculations were performed with the thermodynamic integration procedure (TI).[59] The free energy derivatives were calculated in a vacuum and in water as a function of sampling time (one cumulative calculation each 5 ps) as convergence tests in order to check our protocol for mutation calculations and to improve the accuracy of the selectivity calculations without changing the force field parameters.[45,60] Previously, the MD/FEP method has been used in standard calculations with the protocol 11(1 + 4) ps.[29,37] The equilibration and data collection samplings were fixed and, in the case of convergence problems between two independent mutations, the width of the window, $\delta\lambda$, was changed, leading to mutation lengths varying from 55 ps (11 windows, $\delta\lambda = 0.1$) to 505 ps (101 windows, $\delta\lambda = 0.01$). Based on the hypothesis that the free energy is not a sensitive function of λ, it has been argued that, to obtain a good ratio of sampling length to computational accuracy, it is better to use the molecular dynamics/thermodynamic integration (MD/TI) procedure with a relatively large $\delta\lambda$ and to sample longer in each window in order to minimize the equilibration step and improve sampling for the free energy calculation.[61] The calculation of free energy derivatives for a single λ value (here, $\lambda = 1$) then provides the necessary sampling length at each λ to obtain convergence of each parameter involved in the free energy calculations. For cations, the nonbonded parameters considered are the point charge q, the van der Waals radius R^* and the well depth ε.

The free energy derivatives (FED) for hydrated alkali-metal cations were calculated during 180 ps of MD in water. The evolution of the derivatives as a function of time indicates that a period of 20 ps is necessary to reach convergence for the three derivatives. To discern the impact of the simulation protocol, we calculated ΔG_3 in water for $Na^+ \rightarrow K^+$ and $Rb^+ \rightarrow Cs^+$ mutations (Table 5). The worst results were obtained with the 21(1 + 4) protocol. For the same length of time, the protocol 11(5 + 5) gives a ΔG_3 value closer to the experimental reference. In the simulations with 11 windows, no improvement results in increasing the sampling length beyond 20 ps. The $Rb^+ \rightarrow Cs^+$ mutation overestimates the experimental value by ~0.7 kJ mol^{-1}, while the $Na^+ \rightarrow K^+$ mutation underestimates the target value by ~0.4 kJ mol^{-1}, an inaccuracy which cannot be attributed to the influence of sampling length, as is shown by the unsatisfactory result for the 11(20 + 20) protocol.

For selectivity calculations, the thermodynamic cycle method was considered to be as in Scheme 2[59] where, assuming that

$$\begin{array}{ccc} \text{calix} + M^+ & \xrightarrow{\Delta G_1} & \text{calix}:M^+ \\ \downarrow \Delta G_3 & & \downarrow \Delta G_4 \\ \text{calix} + N^+ & \xrightarrow{\Delta G_2} & \text{calix}:N^+ \end{array}$$

Scheme 2

the system is reversible, the relative binding selectivity is computed by the difference: $\Delta\Delta G = \Delta G_1 - \Delta G_2 = \Delta G_3 - \Delta G_4$. ΔG_3 is calculated in water for the hydrated cations with TI and the protocol 11(2 + 20) ps. The cations were previously equilibrated in a 403 TIP3P water box by a 20 ps MD run.

For ΔG_4 in a vacuum, the cation M^+ is mutated into the cation N^+ by dividing the calculation into 11 intermediate states (windows) defined by a coupling factor λ ($\lambda = 1$ initial state, $\lambda = 0$ final state). In a vacuum, each window was sampled by 52 ps of MD (2 ps equilibration and 50 ps data collection) summarized in the text by 11(2 + 50) ps, or 21(2 + 50) ps in case of convergence problems (mutations between Na^+ and K^+). The value reported is the average value of the two mutations $M^+ \rightarrow N^+$ and $N^+ \rightarrow M^+$. The starting point of each mutation was a structure equilibrated after 100 ps of MD run at 300 K.

Synthesis

Starting materials for synthesis. The solvents and all compounds were commercial reagents and were used without further purification.

Analytical procedures. The melting points (mps) were taken on a Büchi 500 apparatus in capillaries sealed under nitrogen. Silica gel columns were prepared with Kieselgel Merck (N° 11567). Elemental analyses were performed at the *Service de Microanalyse* of the *Institut de Chimie de Strasbourg*. The ^{1}H-NMR spectra were recorded at 200 MHz on a Bruker SY200 spectrometer. The FAB mass spectra were obtained on a VG-Analytical ZAB HF apparatus.

2-(2-Hydroxyethoxy)phenol (1). A mixture of 1,2-dihydroxybenzene (33.03 g, 300 mmol), 2-chloroethanol (24.15 g, 300 mmol), K_2CO_3 (20.75 g, 150 mmol) and acetonitrile (750 ml) was refluxed for 48 h. The mixture was allowed to cool to room temp., filtered and the filtrate concentrated by evaporation under reduced pressure. The residue was chromatographed on a silica column using 80 : 20 $CHCl_3$–acetone as eluent to afford **1** (18.50 g, 40%) as a white solid, mp 102–103 °C. ^{1}H-NMR δ 6.99–6.78 (m, 4H), 4.16–4.11 (m, 2H), 4.03–3.98 (m, 2H), 2.79 (s large, 2H). Anal. Calc. for $C_8H_{10}O_3$: C, 62.33; H, 6.54. Found: C, 62.21; H, 6.59%.

1,2-Bis(2-ethoxyphenyloxy)ethane (2). A mixture of **1** (7.71 g, 50 mmol), K_2CO_3 (69.12 g, 500 mmol), 1,2-dibromoethane (5.64 g, 30 mmol) and acetonitrile (750 ml) was refluxed for 4 days. After cooling to room temp., solvents were removed by evaporation under reduced pressure. The residue was mixed with CH_2Cl_2 and water and neutralized with 1 M HCl. The organic layer was dried over Na_2SO_4, filtered and evaporated on a rotary evaporator. The crude product was chromatographed using 85 : 15 CH_2Cl_2–acetone as eluent to give **2** (4.20 g, 50%) as a white solid, mp 76–77 °C. ^{1}H-NMR δ 6.97 (s, 8H), 4.40–4.34 (m, 6H), 4.14–4.10 (m, 4H), 3.89–3.86 (m, 4H). Anal. Calc. for $C_{18}H_{22}O_6$: C, 64.66; H, 6.63. Found: C, 64.48; H, 6.52%.

Ditosylate of 1,2-bis(2-ethoxyphenyloxy)ethane (3). A mixture of **2** (2.08 g, 6 mmol), toluene-*p*-sulfonyl chloride (2.35 g, 12 mmol) and CH_2Cl_2 (70 ml) was cooled at 0 °C. Then, NEt_3 (2.34 g, 22 mmol) was added dropwise and the reaction mixture was stirred for 48 h. It was then neutralized to pH 1 by addition of 1 M HCl, dried over Na_2SO_4, filtered and evaporated on a rotary evaporator. The crude product was chromatographed using 95 : 5 CH_2Cl_2–acetone as eluent to give **3** (2.42 g, 63%) as a white solid, mp 95–96 °C. ^{1}H-NMR δ 7.77 (d, $J = 8.5$ Hz, 4H), 7.28 (d, $J = 8.5$ Hz, 4H), 6.97–6.81 (m, 8H), 4.31–4.27 (m, 8H), 4.20–4.16 (m, 4H), 2.40 (s, 6H). Anal. Calc. for $C_{32}H_{34}O_{10}S_2$: C, 59.80; H, 5.33. Found: C, 59.71; H, 5.27%.

Calix[4]arene-bis(dibenzo)crown-6 (BC6B2). A mixture of calix[4]arene (0.425 g, 1 mmol), K_2CO_3 (1.382 g, 10 mmol) and acetonitrile (100 ml) was stirred at room temp. for 4 h. Then, the ditosylate **3** (0.643 g, 1 mmol) was added and the mixture was allowed to reflux for 7 days. The same quantities of K_2CO_3 and ditosylate **3** were then added to the mixture which was refluxed for 7 additional days. The solvents were evaporated on a rotatory evaporator and the residue was solubilized in CH_2Cl_2 and neutralized to pH 1 by addition of 1 M HCl. The organic layer was dried over Na_2SO_4, filtered and evaporated. The crude product was chromatographed using 90 : 10 CH_2Cl_2–acetone as eluent to give **BC6B2** (0.850 g, 83%) as a white solid, mp 142–143 °C. ^{1}H-NMR δ 7.14–7.08 (m, 8H), 6.96–6.89 (m, 8H), 6.97–6.81 (m, 8H), 6.72 (d, $J = 7.0$ Hz, 8H), 6.58 (t, $J = 7.0$ Hz, 4H), 4.39 (s, 8H), 3.74 (s, 8H), 3.49 (m, 16H). −MS(FAB$^+$); *m*/*z*: 1021.5 (100%). Anal. Calc. for $C_{64}H_{60}O_{12}$: C, 75.28; H, 5.92. Found: C, 75.18; H, 5.88%.

X-Ray crystallography

BC6B2·CH_3NO_2 1.† *Preparation of single crystals.* Beautiful colorless single crystals suitable for X-ray crystallography were obtained by slow evaporation of a solution of **BC6B2** in nitromethane.

Crystal data. $O_{14}N_1C_{65}H_{63}$, $M_r = 1082.23$, crystallizes in the monoclinic space group $P2_1/n$, $a = 12.260(3)$, $b = 16.998(3)$, $c = 27.624(7)$ Å, $\beta = 102.50(2)°$, $U = 5620(4)$ Å^3, $Z = 4$, $D_c = 1.279$ g cm^{-3}, $\mu = 0.838$ cm^{-1}, $F(000) = 2288$.

Data collection, structure determination and refinement. A parallelepipedic single crystal (dimensions 0.64 × 0.56 × 0.32 mm) was sealed in a glass capillary. The cell constants were obtained from the least-squares refinement of the setting angles of 25 reflections in the range $8 < \theta < 12°$. The data were collected with an Enraf-Nonius CAD4 diffractometer using graphite monochromated MoKα radiation (0.71073 Å) in the range $1 < \theta < 20°$, at room temperature, in the ω/θ scan mode. 2848 reflections with $I > 3\sigma(I)$, out of 5243 unique reflections measured, were used after Lorentz-polarization correction. The intensity decay was not significant and no absorption correction was done. The main part of the structure was solved by direct methods with SHELXS-86,[63] and the remaining atoms were found from subsequent Fourier differences. Oxygen atoms and the atoms of the solvent molecule were refined anisotropically. Hydrogen atoms were included at calculated positions and constrained to ride on their parent carbon atoms (C–H 0.95 Å, isotropic displacement parameter *B* 6 Å^2). Analytical scattering factors for neutral atoms were corrected for $\Delta f'$ and $\Delta f''$. Refinement of 401 parameters was done by full-matrix least-squares on *F* and led to a final conventional *R*1 value of 0.072 ($R1_w = 0.091$, $w = 1/\sigma(F)^2$). The goodness of fit was $S = 3.7$ and the highest and lowest residual densities 0.56 and −0.09 e Å^{-3}. All calculations were performed on a VAX 4000-200 computer with the Enraf-Nonius MolEN system.[64] The molecular drawing was done with ORTEPII.[65]

$Cs_2(NO_3)_2$BC6B2·$CHCl_3$·H_2O 2. *Preparation of single crystals.* **BC6B2** (0.2 mmol) was reacted with $CsNO_3$ (large excess: 2.7 mmol) in $CHCl_3$–CH_3CN (1 : 1, 10 ml) at 65 °C for two days. The remaining $CsNO_3$ was removed by filtration and the solution was allowed to slowly evaporate, leading to beautiful colorless single crystals suitable for X-ray crystallography.

Crystal data. $Cs_2Cl_3O_{19}N_2C_{65}H_{63}$, $M_r = 1548.34$, crystallizes in the monoclinic space group $P2_1/n$, $a = 13.800(1)$, $b =$

† Full crystallographic details for **1** and **2**, excluding structure factor tables, have been deposited at the Cambridge Crystallographic Data Centre (CCDC). For details of the deposition scheme, see 'Instructions for Authors', *J. Chem. Soc.*, *Perkin Trans. 2*, available *via* the RSC web page (http://www.rsc.org/authors). Any request to the CCDC for this material should quote the full literature citation and the reference number 188/151.

24.636(4), $c = 18.735(1)$ Å, $\beta = 102.20(1)°$, $U = 6226(2)$ Å^3, $Z = 4$, $D_c = 1.652$ g cm^{-3}, $\mu = 1.377$ cm^{-1}, $F(000) = 3120$.

Data collection, structure determination and refinement. A parallelepipedic single crystal (dimensions 0.25 × 0.20 × 0.20 mm) was sealed in a glass capillary. The cell constants were determined and the data collected with a Nonius Kappa-CCD diffractometer using graphite monochromated MoKα radiation (0.71073 Å) in the range $1 < \theta < 24.6°$, at 173 K, with 1° steps for the φ scan, 60 second frame intervals and a 28 mm crystal to detector distance. The data were processed with the HKL package (DENZO, XDisplayF, Scalepack).[66] No absorption correction was done. 6474 unique reflections were used. The main part of the structure was solved by direct methods with SHELXS-86,[63] and the remaining atoms were found from subsequent Fourier differences. All non hydrogen atoms were refined anisotropically. Hydrogen atoms were included at calculated positions and constrained to ride on their parent carbon atoms with a displacement factor equal to 1.2 times that of the parent atom. Analytical scattering factors for neutral atoms were corrected for $\Delta f'$ and $\Delta f''$. Refinement of 820 parameters was done by full-matrix least-squares on F^2 and led to final conventional values $R1 = 0.037$ (all reflections, 0.030 for 5641 "observed" ($I > 2\sigma(I)$) ones) and $wR2 = 0.107$ (all reflections, 0.088 for "observed" ones), with $w = 1/[\sigma^2(F_o^2) + (0.1302P)^2 + 71.6189P]$, where $P = (F_o^2 + 2F_c^2)/3$. The goodness of fit was $S = 0.54$ and the highest and lowest residual densities were 0.63 and −0.53 e Å^{-3}. All calculations were performed on a Silicon Graphics Indy station with the SHELXTL system.[67] The molecular drawing was done with ORTEPII.[65]

Picrate extraction experiments

The percentages of alkali picrates extracted from water into dichloromethane (E) have been determined at 20 °C according to the Pedersen's procedure.[68] The experimental details and the preparation of the metal picrates have already been reported.[69]

Stability constant in acetonitrile

The stability constants, expressed as the concentration ratios $\beta_{xy} = [M_xL_y^{x+}]/[M^+]^x[L]^y$ and corresponding to the overall equilibrium: $xM^+ + yL \rightleftharpoons M_xL_y^{x+}$ have been determined in acetonitrile (SDS, purex for Analyses), **BC6B2** not being soluble enough in methanol. The measurements were performed by UV-absorption spectrophotometry. The procedure was identical to that already described.[18] As the equilibria were reached rapidly, titration of the ligand ($C_L = 2–8 \times 10^{-5}$ M) by the metal ion solution was performed directly in the spectrophotometric cell. The final ratio $R = C_M/C_L$ of the concentration of metal to the concentration of ligand was adjusted in order to obtain the maximum spectral changes. In the case of very weak complexation, as for Li^+ and Na^+ cations, values of R higher than 900 were used. The spectra were recorded between 250 and 300 nm, at 25 °C, with a Shimadzu UV-2101-PC spectrophotometer after each addition of metal salt. As far as possible, the ionic strength was maintained at 0.01 M in all solutions by the use of Et_4NClO_4. The metal salts were the following perchlorates: $NaClO_4$ (Fluka, purum), $KClO_4$ (Prolabo, Normapur), $RbClO_4$ (Sigma) and caesium nitrate: $CsNO_3$ (Merck). All these salts were dried under vacuum for 12 h before use. The spectral changes recorded have been interpreted by the program Sirko.[70]

Thermodynamic parameters in acetonitrile

The enthalpies of complexation ΔH_{xy} have been determined by calorimetric titrations using a Tronac isoperibolic calorimeter. The procedure has been reported in detail elsewhere.[71] Solutions of the metal salts were titrated into solutions of the ligand (2.5×10^{-4} M $\leq C_L \leq 10^{-3}$ M). For solubility reasons, the metal iodides were used instead of the perchlorates used for spectrophotometric measurements: KI (Prolabo, p.a.), RbI (Merck, Suprapur) and CsI (Janssen Chimica). ΔH_{xy} values were refined using the program Sirko,[70] the stability constants obtained by spectrophotometry being taken as constant. The corresponding entropies of complexation ΔS_{xy} were then derived from the expression $\Delta G_{xy} = \Delta H_{xy} - T\Delta S_{xy}$.

Association constants in THF

Spectrophotometric titrations in tetrahydrofuran (THF) have been performed according to Smid's procedure[72] as described earlier.[48] Increasing amounts of ligand solution in THF (SDS, Analytical Grade) were added to 1 ml of metal picrate in THF, directly in the spectrophotometric cell. After each addition of ligand the spectra were recorded between 300 and 500 nm on a Shimadzu UV-2101-PC spectrophotometer using supracil cuvettes of 0.5 cm path length and thermoregulated at 25 °C. The experimental spectra were treated by the program Sirko[70] as follows: the molar absorptivities and the association constants K_a of the species formed, corresponding to the following equilibria: $M^+Pic^- + L \rightleftharpoons MLPic$, were first refined simultaneously from the absorbances at ten significant wavelengths where the greatest changes occurred. Then, the molar absorptivities at several wavelengths, chosen every nm around the expected maximum, were refined in order to determine the position of the maximum absorption of the complexes. The association constants obtained from the first refinement were taken as constant during this treatment.

Acknowledgements

V. L. thanks COGEMA for financial support. S. F. thanks the French Government and SFERE (Société Française d'Exportation des Ressources Educatives) for a grant.

References

1 *Chemical Separations with Liquid Membranes*, R. A Bartsch and J. D. Way Eds., ACS Symposium Series 642, American Chemical Society, 1996.
2 *New Separation Chemistry Techniques for Radioactive Waste and Other Specific Applications*, L. Cecille, M. Casarci and L. Pietrelli Eds., Elsevier Applied Science, London and New York, 1991.
3 *Future Industrial Prospects of Membrane Processes*, L. Cecille and J.-C. Toussaint Eds., Elsevier Applied Science, London and New York, 1989.
4 *Supramolecular Chemistry*, J.-M. Lehn Ed., VCH, Weinheim, 1995.
5 B. A. Moyer and Y. Sun, in *Ion Exchange and Solvent Extraction*, J. A. Marinsky and Y. Marcus Eds., Marcel Dekker Inc., 1997, Vol. 13, Chap. 6, pp. 295–391.
6 M. Bourgeois, in *Techniques de l'Ingénieur*, Traité Mécanique et Chaleur, B 3650.
7 T. J. Haverlock, P. V. Bonnesen, R. A. Sachleben and B. A. Moyer, *Radiochim. Acta*, 1997, **76**, 103
8 C. D. Gutsche, *Calixarenes*, Royal Society of Chemistry, Cambridge, 1989.
9 *Calixarenes: a Versatile Class of Macrocyclic Compounds*, J. Vicens and V. Böhmer Eds., Kluwer Academic Publishers, Dordrecht, 1991.
10 V. Böhmer, *Angew. Chem., Int. Ed. Engl.*, 1995, **34**, 713.
11 Z. Asfari, S. Wenger and J. Vicens, *Supramol. Sci.*, 1994, **1**, 103.
12 Z. Asfari, S. Wenger and J. Vicens, in *Calixarenes' 50th Anniversary*, J. Vicens, Z. Asfari and J. M. Harrowfield Eds., Kluwer Academic Publishers, 1995, pp. 137-148. Reprinted from *J. Inclusion Phenom. Mol. Recognit. Chem.*, 1994, **19**, 137.
13 Z. Asfari, S. Wenger and J. Vicens, *Pure Appl. Chem.* 1995, **67**, 1037.
14 Z. Asfari, M. Nierlich, P. Thuéry, V. Lamare, J.-F. Dozol, M. Leroy and J. Vicens, *Anal. Quím. Int. Ed.*, 1996, **92**, 260.
15 C. Hill, J.-F. Dozol, V. Lamare, H. Rouquette, S. Eymard, B. Tournois, J. Vicens, Z. Asfari, C. Bressot, R. Ungaro and A. Casnati, in *Calixarenes' 50th Anniversary*, J. Vicens, Z. Asfari and J. M. Harrowfield Eds., Kluwer Academic Publishers, 1995, pp. 399–408. Reprinted from *J. Inclusion Phenom. Mol. Recognit. Chem.*, 1994, **19**, 399.
16 Z. Asfari, C. Bressot, J. Vicens, C. Hill, J.-F. Dozol, H. Rouquette, S. Eymard, V. Lamare and B. Tournois, *Anal. Chem.*, 1995, **67**, 3133.
17 Z. Asfari, C. Bressot, J. Vicens, C. Hill, J.-F. Dozol, H. Rouquette, S. Eymard, V. Lamare and B. Tournois, in *Chemical Separations*

with Liquid Membranes, R. A. Bartsch and J. D. Way Eds., ACS Symposium Series 642, American Chemical Society, 1996, pp. 376–390.
18 F. Arnaud-Neu, Z. Asfari, B. Souley and J. Vicens, *New J. Chem.*, 1996, **20**, 453.
19 A. D'Aprano, J. Vicens, Z. Asfari, M. Salomon and M. Iammarino, *J. Solution Chem.*, 1996, **25**, 955.
20 P. Thuéry, M. Nierlich, C. Bressot, V. Lamare, J.-F. Dozol, Z. Asfari and J. Vicens, *J. Inclusion Phenom. Mol. Recognit. Chem.*, 1996, **23**, 305.
21 Z. Asfari, C. Naumann, J. Vicens, M. Nierlich, P. Thuéry, C. Bressot, V. Lamare and J.-F. Dozol, *New J. Chem.*, 1996, **20**, 1183.
22 P. Thuéry, M. Nierlich, Z. Asfari and J. Vicens, *J. Inclusion Phenom. Mol. Recognit. Chem.*, 1997, **27**, 169.
23 P. Thuéry, M. Nierlich, J. C. Bryan, V. Lamare, J.-F. Dozol, Z. Asfari and J. Vicens, *J. Chem. Soc., Dalton Trans.*, 1997, 4191 (and references therein).
24 P. Thuéry, M. Nierlich, V. Lamare, J.-F. Dozol, Z. Asfari and J. Vicens, *Supramol. Chem.*, 1997, **8**, 319.
25 R. Ungaro, A. Casnati, F. Ugozzoli, A. Pochini, J.-F. Dozol, C. Hill and H. Rouquette, *Angew. Chem., Int. Ed. Engl.*, 1994, **33**, 1506.
26 F. Ugozzoli, O. Ori, A. Casnati, A. Pochini, R. Ungaro and D. N. Reinhoudt, *Supramol. Chem.*, 1995, **5**, 179.
27 A. Casnati, A. Pochini, R. Ungaro, F. Ugozzoli, F. Arnaud, S. Fanni, M.-J. Schwing, R. J. M. Egberink, F. de Jong and D. N. Reinhoudt, *J. Am. Chem Soc.*, 1995, **117**, 2767.
28 F. Arnaud-Neu, N. Deutsch, S. Fanni, M. J. Schwing-Weill, A. Casnati and R. Ungaro, *Gazetta Chim. Ital.*, 1997, **127**, 693.
29 G. Wipff and M. Lauterbach, *Supramol. Chem.*, 1995, **6**, 187.
30 A. Varnek and G. Wipff, *J. Mol. Struct.* (*THEOCHEM*), 1996, **363**, 67.
31 G. Wipff, E. Engler, P. Guilbaud, M. Lauterbach, L. Troxler and A. Varnek, *New J. Chem.*, 1996, **20**, 403.
32 M. Lauterbach and G. Wipff, in *Physical Supramolecular Chemistry*, NATO ASI series, L. Echegoyen and A. Kaifer Eds., Kluwer, Dordrecht, 1996, pp. 1–38.
33 A. Varnek and G. Wipff, *J. Comput. Chem.*, 1996, **17**, 1520.
34 M. Lauterbach, E. Engler, N. Muzet, L. Troxler and G. Wipff, *J. Phys. Chem. B*, 1998, **102**, 245.
35 M. Lauterbach, G. Wipff, A. Mark and W. van Gunsteren, *Gazetta Chim. Ital.*, 1997, **127**, 699.
36 C. Bressot, PhD Thesis, Université Louis Pasteur de Strasbourg, France, 1995.
37 V. Lamare, C. Bressot, J.-F. Dozol, J. Vicens, Z. Asfari, R. Ungaro and A. Casnati, *Sep. Sci. Technol.*, 1997, **32**, 175.
38 J. Aqvist, *J. Phys. Chem.*, 1990, **94**, 8021.
39 S. Miyamoto and P. A. Kollman, *J. Am. Chem. Soc.*, 1992, **114**, 3668.
40 T. Kowall and A. Geiger, *J. Phys. Chem.*, 1994, **98**, 6216.
41 P. D. J. Grootenhuis and P. A. Kollman, *J. Am. Chem. Soc.*, 1989, **111**, 2152.
42 J. Marrone, D. S. Hartsough and K. M. Merz, *J. Phys. Chem.*, 1994, **98**, 1341.
43 V. Lamare, J.-F. Dozol, F. Ugozzoli, A. Casnati and R. Ungaro, *Eur. J. Org. Chem.*, 1998, 1559.
44 D. J. Cram, *Angew. Chem., Int. Ed. Engl.*, 1998, **27**, 1009.
45 P. Cieplak, D. A. Pearlman and P. A. Kollman, *J. Chem. Phys.*, 1994, **101**, 627.
46 ^{1}H-NMR spectra of Cs^+ and Rb^+ complexes of **BC6B2** show important modifications in the region of the protons belonging to the benzo substituents as compared to the free ligand, which may be attributed to π–cation interactions. Such modifications are not visible in the spectrum of the K^+ complex. On the other hand, the spectra of Cs^+, Rb^+ and K^+ complexes of **BC6N** do not show any modification in the naphthalene region with respect to the free **BC6N**.[23]
47 R. M. Izatt, J. S. Bradshaw, S. A. Nielsen, J. D. Lamb, J. J. Christensen and D. Sen, *Chem. Rev.*, 1985, **85**, 271.
48 F. Arnaud-Neu, Z. Asfari, B. Souley and J. Vicens, *Anal. Quím. Int. Ed.*, 1997, **93**, 404.
49 J.-F. Dozol, V. Lamare, C. Bressot, R. Ungaro, A. Casnati, J. Vicens and Z. Asfari, Fr. Pat. 97 02490.
50 C. Sorel, PhD Thesis, Université Paris VI, France, 1996.
51 J.-F. Dozol, N. Simon, V. Lamare, H. Rouquette, S. Eymard, B. Tournois and D. De Marc, Poster presented at *10th Symposium on Separation Science and Technology for Energy Applications*, Gatlinburg, Tennessee, October 20–24, 1997 (accepted in *Sep. Sci. Technol.*).
52 B. F. Myasoedov, M. K. Chmutova, N. E. Kochetkova, O. E. Koiro, G. A. Pribylova, N. P. Nesterova, T. Ya. Medved and M. I. Kabachnik, *Solvent Extr. Ion Exch.*, 1986, **4**, 61.
53 R. Chiarizia and E. P. Horwitz, *Solvent Extr. Ion Exch.*, 1992, **10**, 101.
54 M. N. Litvina, M. K. Chmutova, B. F. Myasoedov and M. I. Kabachnik, *Radiochemistry*, 1996, **38**, 494.
55 D. A. Pearlman, D. A. Case, J. A. Caldwell, W. S. Ross, T. E. Cheatham III, D. M. Ferguson, G. L. Seibel, U. C. Singh, P. Weiner and P. A. Kollman, AMBER 4.1, University of California, San Francisco, 1995.
56 S. J. Weiner, P. A. Kollman, D. T. Nguyen and D. A. Case, *J. Comput. Chem.*, 1986, **7**, 230.
57 Insight II, Biosym Technologies, 1993.
58 E. Engler, G. Wipff, MDS. Université Louis Pasteur, Strasbourg, France, 1992; E. Engler and G. Wipff, in *Crystallography of Supramolecular Compounds*, G. Tsoucaris Ed., Kluwer, Dordrecht, 1996, pp. 471–476.
59 P. A. Kollman, *Chem. Rev.*, 1993, **93**, 2395.
60 D. A. Pearlman, *J. Comput. Chem.*, 1994, **15**, 105.
61 T. P. Straatsma and H. J. C. Berendsen, *J. Chem. Phys.*, 1988, **89**, 5876.
62 Y. Marcus, *Chem. Rev.*, 1988, **88**, 1475.
63 G. M. Sheldrick, SHELXS-86: Program for the Solution of Crystal Structures, University of Göttingen, 1985.
64 *MolEN: An Interactive Structure Solution Procedure*, Enraf-Nonius, Delft, 1990.
65 C. K. Johnson, ORTEPII, Report ORNL-5138, Oak Ridge National Laboratory, Tennessee, 1976.
66 Z. Otwinowski and W. Minor, *Processing of X-ray Diffraction Data Collected in Oscillation Mode*, in *Methods in Enzymology*, *Vol. 276: Macromolecular Crystallography*, *Part A*, pp. 307–326, C. W. Carter, Jr. and R. M. Sweet Eds., Academic Press, 1997.
67 SHELXTL, version 5.03, Analytical X-ray Systems, Karlsruhe, 1997.
68 C. J. Pedersen, *Fed. Proc. Fed. Am. Soc. Expl. Biol.*, 1968, **27**, 1305.
69 F. Arnaud-Neu, M. J. Schwing-Weill, K. Ziat, S. Cremin, S. J. Harris and M. A. McKervey, *New J. Chem.*, 1991, **15**, 33.
70 V. Vetrogon, N. G. Lukyanenko, M. J. Schwing-Weill and F. Arnaud-Neu, *Talanta*, 1994, **41**, 2105.
71 F. Arnaud-Neu, G. Barrett, S. Fanni, D. Marrs, W. McGregor, M. A. McKervey, M. J. Schwing-Weill, V. Vetrogon and S. Wechsler, *J. Chem. Soc., Perkin Trans. 2*, 1995, 453.
72 M. Bourgoin, K. H. Wong, J. Y. Hui and J. Smid, *J. Am. Chem. Soc.*, 1975, **97**, 3462.

Paper 8/06714G